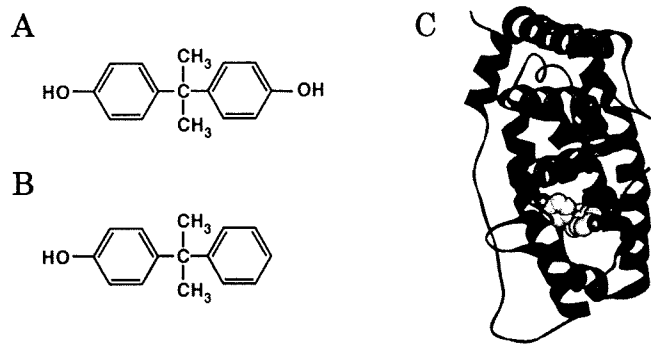

Fig. 1. Chemical structures of bisphenol A (A) and 4-α-cumylphenol(B). Overall structure of 4-α-cumylphenol/ERRγ complex (C).

Results and Discussion

ERRγ was expressed in *E. coli* BL21 as glutathione *S*-transferase (GST) fusion protein. The protein expressed was affinity-purified by using glutathione Sepharose resin, and GST was enzymatically cleaved. The resulting protein was crystallized in the presence of 4-α-cumylphenol. The X-ray crystal structural analysis was performed, and 4-α-cumylphenol/ERRγ complex structure was resolved by molecular replacement method using BPA/ERRγ complex as the searching model. The final model was refined at a 2.0 Å resolution.

The overall structure of 4-α-cumylphenol/ERRγ complex features 12 α-helices (H1-H12) and 2 β-strands in a sheet (S1) without any disordered amino acid residues, and the amino acid residues in the binding pocket were found to be almost the same as those in the BPA/ERRγ complex. Two hydrogen bonds were formed between the remaining OH group of 4-α-cumylphenol and Glu275 or Arg316. Another hydrogen bond of the second BPA-phenol-OH is formed with Asn346 of ERRγ-LBP. Since 4-α-cumylphenol lacks this phenol-OH groups, it should hold substitute residues for a strong receptor binding. When we superimposed the 4-α-cumylphenol/ERRγ-LBD complex with the BPA/ERRγ-LBD complex, we found that the Leu345-isobutyl group rotates 180° completely around the $_{\alpha}C$-$_{\beta}C$ bond. ERRγ changes its conformation of Leu345 side chain by the back-and-forth rotation to receive either phenol (BPA) or phenyl (4-α-cumylphenol). Since the Leu conformation in the 4-α-cumylphenol complex was found to be the same as in the apo-form, it become evident that that Leu345 does made a rotation of about 180° to adopt the phenol group of BPA. The crystal structure of the ERRγ complex with (or without) chemicals clearly revealed that ERRγ's Leu345-β-isoprorpyl plays a role in the tight binding of 4-α-cumylphenol and BPA, rotating in a back-and-forth induced-fit manner.

References

1. Takayanagi, S. Tokunaga, T., Liu, X., Okada, H., Matsushima, A., and Shimohigashi, Y. (2006) *Toxicol. Lett.*, **167**, 95-105.
2. Okada, H., Tokunaga, T., Lui, X., Takayanagi, S., Matsushima, A., and Shimohigashi, Y. (2008) *Environ. Health Perspect.*, **116**, 32-38.
3. Matsushima, A., Kakuta, Y., Teramoto, T., Koshiba, T., Liu, X., Okada, H., Tokunaga, T., Kawabata, S., Kimura, M., and Shimohigashi, Y. (2007) *J. Biochem.*, **142**, 517-524.
4. Matsushima. A., Teramoto, T., Okada, H., Liu, X., Tokunaga, T., Kakuta, Y., and Shimohigashi, Y. (2008) *Biochem. Biophys. Res. Commun.*, **373**, 408-413.

Peptide Science 2008: M. Nomizu (Ed.)
The Japanese Peptide Society (2009)

Bisphenol A-Specific Nuclear Receptor ERRγ: Structure-Function Analysis of the Two Novel Isoforms Lacking Vital Peptide Fragment in the Ligand Binding Domain

Yukimasa Takeda[1], Xiaohui Liu[1], Miho Sumiyoshi[2], Ayami Matsushima[1], Miki Shimohigashi[2], and Yasuyuki Shimohigashi[1]

[1]Laboratory of Structure-Function Biochemistry, Department of Chemistry, Faculty of Sciences, Kyushu University, Fukuoka 812-8581, Japan, and [2]Division of Biology, Faculty of Science, Fukuoka University, Fukuoka 814-0180, Japan
e-mail: shimo@chem.kyushu-univ.jp

We have demonstrated that ERRγ binds strongly bisphenol A (BPA), one of the nastiest endocrine disruptors, retaining ERRγ's high basal constitutive activity. In the present study, we found the two different LBD-wrecked ERRγ isoforms, which are abundant (about 20%) broadly in various human tissues. These ERRγ isoforms were suggested to affect the sound ERRγ as a regulatory element.

Keywords: bisphenol A, endocrine disruptor, ERRγ, isoforms, nuclear receptor

Introduction

Estrogen-related receptor γ (ERRγ), one of 48 human nuclear receptors, is in a fully activated conformation with no ligand. We have recently demonstrated that ERRγ binds strongly bisphenol A (BPA) with the high basal constitutive activity [1]. In the *in vivo* animal experiments, the low-dose effects of BPA have been evidenced, and thus the adverse effects of ERRγ are very much doubtful. Although we found that human placenta and brain stem express predominantly one of ERRγ mRNA variants, little is known about the intrinsic molecular mechanism of ERRγ functions. In the present study, we revealed the molecular multiplicity of ERRγ mRNAs and proteins, which must be correlated to the multiplicity of physiological functions.

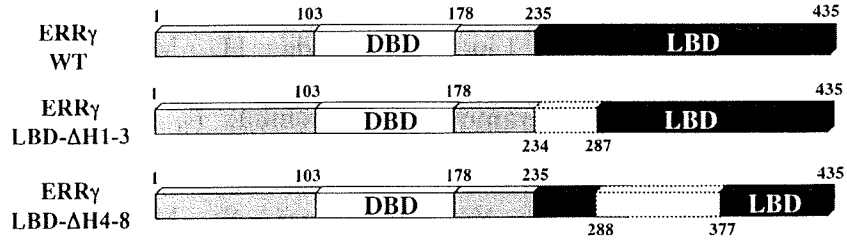

Fig. 1. The three different types of human ERRγ isoforms with wrecked LBD.

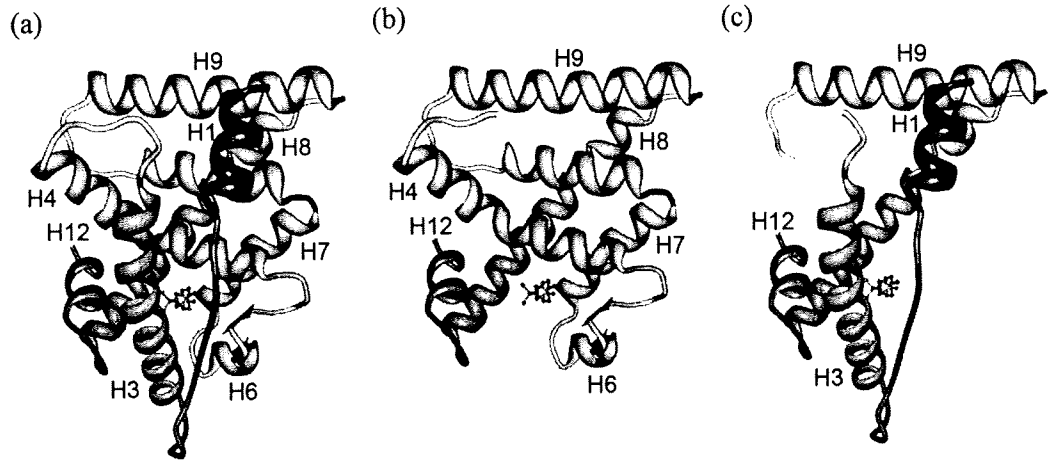

Fig. 2. 3D-Structure of the wild type ERRγ-LBD and its LBD-wrecked forms. (a) ERRγ LBD-WT, (b) ERRγ LBD-ΔH1-3, and (c) ERRγ LBD-ΔH4-8.

Results and Discussion

We eventually identified total 34 mRNA splicing variants from human tissues. As a result, these variants were established to produce 10 protein isoforms. Among these isoforms, two distinct isoforms have a wrecked or broken LBD due to the lack of a peptide fragment either 234-287 or 288-377 (Fig. 1). Those were designated as ERRγ LBD-ΔH1-3 and ERRγ LBD-ΔH4-8, respectively. By means of real-time PCR measurement, these LBD-wrecked isoforms were found to be considerably abundant (3-6% and 12-20%, respectively) broadly in human tissues, suggesting their physiological significance. It should be noted that those do not exhibit any constitute activity in the reporter gene assay.

The LBD of nuclear receptors is constructed by 12 highly conserved α-helix peptides (H1 - H12). Structural evidence for BPA binding to ERRγ-LBD revealed importance of the receptor residues such as Glu275, Arg316, Tyr326, and Asn346 in the ligand-binding pocket [2-4]. The polar amino acids Glu275, Arg316, and Asn346 play central role in forming the hydrogen bonding of two BPA-phenol-OH groups. Surrounding hydrophobic bonds, especially those by Tyr326, reinforce BPA's specific binding. These critical residues are located in H3 (Glu275), H4 (Arg316), and H7 (Asn346), respectively. Tyr326 is in a β-sheet structure located in H4 and H6. As shown in Fig. 2, ERRγ LBD-ΔH1-3 just wrecks H1 and H3, while ERRγ LBD-ΔH4-8 is devoid of the peptide fragment corresponding to H4 - H8. It was strongly suggested that these LBD-broken isoforms cannot bind BPA in their incomplete ligand pockets. Since both isoforms retain H10 essential for functional receptor dimerization, those are probably a regulatory element of sound ERRγ.

References

1. Takayanagi, S., Tokunaga, T., Liu, X., Okada, H., Matsushima, A., and Shimohigashi, Y. (2006) *Toxicol. Lett.*, **167**, 95-105.
2. Matsushima, A., Kakuta, Y., Teramoto, T., Koshiba, T., Liu, X., Okada, H., Tokunaga, T., Kawabata, S., Kimura, M., and Shimohigashi, Y. (2007) *J. Biochem.*, **142**, 517-524.
3. Okada, H., Tokunaga, T., Liu, X., Takayanagi, S., Matsushima, A., and Shimohigashi, Y. (2008) *Environ. Health Perspect.*, **116**, 32-38.
4. Matsushima, A., Teramoto, T., Okada, H., Liu X., Tokunaga, T., Kakuta, Y., and Shimohigashi, Y. (2008) *Biochem. Biophys. Res. Commun.*, **373**, 408-413.

J. Biochem. 2009;146(1)113–122
doi:10.1093/jb/mvp049

Placenta Expressing the Greatest Quantity of Bisphenol A Receptor ERRγ among the Human Reproductive Tissues: Predominant Expression of Type-1 ERRγ Isoform

Yukimasa Takeda[1,*], Xiaohui Liu[1], Miho Sumiyoshi[2], Ayami Matsushima[1], Miki Shimohigashi[2] and Yasuyuki Shimohigashi[1,†]

[1]Laboratory of Structure-Function Biochemistry, Department of Chemistry, The Research- Education Centre of Risk Science, Faculty of Sciences, Kyushu University, Fukuoka 812-8581; and [2]Division of Biology, Faculty of Science, Fukuoka University, Fukuoka 814-0180, Japan

Received February 19, 2009; accepted March 7, 2009; published online March 20, 2009

Estrogen-related receptor γ (ERRγ), one of the 48 human nuclear receptors, has a fully active conformation with no ligand. We recently demonstrated that ERRγ binds strongly bisphenol A (BPA), one of the nastiest endocrine disruptors, and thus retaining ERRγ's high basal constitutive activity. A report that BPA accumulates in the human maternal–fetal placental unit has led us to hypothesize that a large amount of ERRγ might exist in the human placenta. Here we report evidence that placenta indeed expresses ERRγ exceptionally strongly. We first ascertained the presence of nine different ERRγ mRNA variants and the resulting three ERRγ protein isoforms. By real-time PCR, we estimated the relative amount of ERRγ mRNA using total RNA extracts from human reproductive tissues. Placenta was found to express ERRγ extremely highly. Among the three ERRγ protein isoforms, placenta exclusively expresses the type-1 isoform, which possesses additional 23-mer amino-acid residues at the N-terminus of the ordinary ERRγ. This N-terminal elongation was found to elevate by approximately 50% the basal constitutive activity of ERRγ, as evidenced in the luciferase reporter gene assay. The present results suggest that BPA accumulates in the placenta by binding to ERRγ.

Key words: alternative splicing, bisphenol A receptor, estrogen-related receptor γ, placenta, real-time PCR.

Abbreviations: AR, androgen receptor; BPA, bisphenol A; ER, estrogen receptor; ERR, estrogen-related receptor; ERRE, ERR-response element; ERRγ, estrogen-related receptor γ; NRs, nuclear receptors; 4-OHT, 4-hydroxytamoxifen.

INTRODUCTION

Bisphenol A (BPA), 2,2-*bis*(4-hydroxyphenyl)-propane, is one of the highest volume chemicals produced worldwide as a starting material for polycarbonate plastics and epoxy resins. Long known as an estrogenic chemical, BPA is suspected of interacting with human estrogen receptor ER (*1*, *2*) or acting as an antagonist for a human androgen receptor (AR) (*3*, *4*). However, BPA's binding to ER and AR and its hormonal activity are extremely weak: 1,000–10,000 times weaker than with natural hormones.

Based on the idea that BPA may interact with nuclear receptors (NRs) other than ER and AR, we screened a series of nuclear receptors and eventually explored estrogen-related receptor γ (ERRγ) as the BPA target receptor. BPA was found to bind strongly to ERRγ with high constitutive basal activity (*5–7*). BPA's binding to ERRγ was further demonstrated by X-ray crystallographic analysis of the complex between BPA and ERRγ (*8*, *9*).

In our efforts to explore the genuine characteristics of ERRγ as a BPA receptor, we have noticed the presence of several different *ERRγ* mRNA isoforms. NRs often possess a number of mRNA isoforms produced by alternative splicing to exhibit functions in a tissue-specific or developmental stage-specific manner (*10*, *11*). However, little is known about the *in vivo* physiological functions of those splicing variants, and even the variants' tissue distributions are poorly understood.

BPA as an endocrine disruptor poses the worrisome threat of low-dose effects on reproductive and developmental processes in humans (*12*). To ensure the presence of *ERRγ* mRNA isoforms in human reproductive organs and brains, we attempted to quantify the total amount of *ERRγ* mRNAs and then the amount of each mRNA isoform. Here we report evidence that the human placenta expresses *ERRγ* mRNA extremely highly, and that the class of isoforms is type-1 ERRγ.

MATERIALS AND METHODS

cDNA Cloning—To confirm the presence of eight reported isoforms of *ERRγ* mRNA, we cloned cDNA by

*Present address: Cell Biology Section, Laboratory of Respiratory Biology, NIH-NIEHS, Research Triangle Park, NC 27709, USA.
†To whom correspondence should be addressed. Tel/Fax: +81-92-642-2584, E-mail: shimo@chem.kyushu-univ.jp

using human pancreas and skeletal muscle. These total RNA samples (Clontech, Mountain View, CA, USA) were reverse-transcribed by using the forward primer of ERRγRT1 (5′-GAAAGCTGCTTCATAGTCTTGCTG-3′) and the enzyme SuperScriptII™ RNase H⁻ Reverse Transcriptase (Invitrogen, Carlsbad, CA, USA) at 42°C.

To confirm that all clones had inconsistent 5′-UTR sequences, the forward primers were designed separately, depending on the unique structure of each exon (Table 1). As reverse primers, ChERRγR1 and ChERRγR2 were used in the first and the nested PCRs, respectively. As for the amplification of *ERRγ1* cDNA, the first PCR was carried out using a primer set of ChERRγ1F/ChERRγR1 and the enzyme *Pfu Turbo*® Hotstart DNA Polymerase (Stratagene, La Jolla, CA, USA). The second PCR was performed by using PLATINUM® *Taq* DNA polymerase (Invitrogen) with another primer set of ChERRγ1F/ChERRγR2 and the product from the first PCR as a template. For amplification of all other *ERRγ*, PCR was carried out by the same method. Sequence analysis was carried out on CEQ8800 Genetic Analysis System (Beckman Coulter, Fullerton, CA, USA).

Real-Time PCR—The total RNA samples extracted from brains (adult and fetal) and various different reproductive tissues (ovary, uterus, placenta, prostate and testis) were purchased from Clontech, Stratagene and Biochain (Hayward, CA, USA). Each total RNA sample (1 μg) was reverse-transcribed by using SuperScriptII™ (Invitrogen) and oligonucleotide ERRγRT2 (5′-GGAGCAGTCATCATACAG-3′) and hgapdhRT (5′-ATGGTACATGACAA GGTG-3′).

Table 1. **The oligonucleotide sequences of primers used for cDNA cloning of a series of ERRγ mRNA isoform.**

Name of primers	Oligonucleotide sequences
Primers for amplification of ERRγ1 cDNA	
ChERRγ1F	5′-CTGTGCTCTGTCAAGGAAACTTTG-3′
ChERRγR1[a]	5′-GAAAGCTGCTTCATAGTCTTGCTG-3′
ChERRγR2[b]	5′-TTTCAACATGAAGGATGGGAAG-3′
Primers for amplification of ERRγ2 cDNA	
ChERRγ2F	5′-TACGCTAACACTGTCGCAGTTTG-3′
ChERRγ2-adF1	5′-GGTTTTGTAGACTTTCATAGCCAAAG-3′
ChERRγ2-adF2	5′-CGACTCACCTGATTAACCTGCTG-3′
ChERRγR1[a]	5′-GAAAGCTGCTTCATAGTCTTGCTG-3′
ChERRγR2[b]	5′-TTTCAACATGAAGGATGGGAAG-3′
Primers for amplification of ERRγ2-gig cDNA	
ChERRγ2-gigF1	5′-GCCACCACATCTCGATTCAAAG-3′
ChERRγ2-gigF2	5′-CACATGTTCGTGGTGTGGAAAG-3′
ChERRγR1[a]	5′-GAAAGCTGCTTCATAGTCTTGCTG-3′
ChERRγR2[b]	5′-TTTCAACATGAAGGATGGGAAG-3′
Primers for amplification of ERRγ3 cDNA	
ChERRγ3F1	5′-CGGTCCTTCACTTGGAGTTAGTG-3′
ChERRγ3F2	5′-CAAGCTTTATATAGGATCACCGTTGTG-3′
ChERRγR1[a]	5′-GAAAGCTGCTTCATAGTCTTGCTG-3′
ChERRγR2[b]	5′-TTTCAACATGAAGGATGGGAAG-3′
Primers for insertion/deletion confirmation of exon K	
ChERRγJF	5′-CAGAATGTCAAACAAAGATCGACAC-3′
ChERRγLR	5′-CAGCTGAGGGTTCAGGTATGG-3′

[a]The antisense reverse primer R1 has the same nucleotide sequence.
[b]The antisense reverse primer R2 has the same nucleotide sequence.

Real-time PCR was performed on a capillary-type LightCycler™ rapid thermal cycler system (Roche Diagnostics, Mannheim, Germany). Reactions were completed in a 10 μl solution mixture and SYBR Green Realtime PCR Master Mix (Toyobo, Tokyo). For normalization, the mRNA gene (*gapdh*) of the enzyme glyceraldehyde-phosphate dehydrogenase was amplified as an internal standard. The assay includes the steps of denaturation at 95°C for 1 min, annealing at 61°C for 3 s and extension at 72°C for a variable time, depending upon the size of products. The product specificity was always confirmed by agarose gel electrophoresis and routinely estimated by the melting curve analysis. To depict the standard curves for quantitative real-time PCR, a 10^{-1}-fold series of dilutions of each plasmid with the same DNA sequence was simultaneously amplified. Quantification of mRNA was achieved using LightCycler software (version 3.5). Standard curves had a correlation coefficient (r^2) of 1.00, linear over a sample concentration range, and mean square error values of 0.03–0.08 were involved.

Western Blotting Analyses—Western blotting was used to detect ERRγ protein isoforms from human kidney and placenta. ERRγ-specific mouse monoclonal antibody was purchased from Perseus Proteomics (Tokyo). The human placenta and kidney lysates were purchased from ProSci (Poway, CA, USA). These lysates (20 μg each) was electrophoresed on 10% polyacrylamide gels. After electrophoresis, gels were electro-blotted onto Hybond-P (GE Healthcare, Waukesha, WI, USA). The blot was incubated overnight in the presence of the anti-ERRγ monoclonal antibody. ERRγ protein was visualized by chemi-luminescence (GE Healthcare) using HRP-conjugated secondary antibody (Jackson ImmunoResearch, West Grove, PA, USA). To discriminate a positive band from negative ones, negative staining controls were performed without the first antibodies.

Reporter Gene Assay for ERRγ Types 1 and 2—Type I and type II ERRγ fragments were cloned into the vector pcDNA3.1(+) (Invitrogen). As an ERR response element (ERRE)-luciferase construct, 3 × ERRR/pGL3 was used as described previously (7). HeLa cells were maintained in Eagle's MEM medium (Nussui, Tokyo) with 10% (v/v) fetal bovine serum at 37°C. HeLa cells were transfected with 3 μg of luciferase reporter gene (pGL3/3 × ERRE), 1 μg of the expression plasmid of the wild-type of either type I or type II ERRγ and 10 ng pSEAP-control plasmid as an internal control by Lipofectamine Plus reagent (15 μl/ml, Invitrogen). Approximately 24 h after transfection, cells were harvested and plated into 96-well plates at a concentration of 5×10^4 cells/well. The cells were then treated with varying doses of chemicals, BPA (Tokyo Kasei Kogyo, Tokyo) and 4-OHT (Sigma-Aldrich, St. Louis, MO, USA), diluted with 1% BSA/PBS (v/v). After 24 h, luciferase activity was measured by using the Luciferase assay reagent (Promega, Madison, WI). SEAP activity was assayed by using Great EscAPe™ SEAP assay reagent (Clontech) according to the Fluorescent SEAP Assay protocol. Light emission was measured on a microplate reader Wallac 1420 ARVOsx (Perkin Elmer, Turku, Finland). Cells treated with 1% BSA/PBS were

used as a vehicle control. Each assay was performed in duplicate and repeated at least three times.

RESULTS

Confirmation and Classification of Alternative Splicings of ERRγ Gene—To date, three independent investigations have revealed six alternative splicing sites for the human *ERRγ* mRNA gene and eight different *ERRγ* mRNA variants (*13–15*). However, there is no systematic study to unify these results, and thus it is unclear whether or not all of these variants are present simultaneously in one species, such as humans. Thus, we first attempted to confirm the full-length sequences of cDNAs derived from the eight *ERRγ* mRNA splicing variants.

To amplify each *ERRγ* mRNA isoform—*ERRγ1*, *ERRγ2*, *ERRγ2-gig* and *ERRγ3*—PCR was conducted successfully by using a series of forward sense and reverse antisense primer sets was designed for each isoform (Table 1) and commercially available pancreas and skeletal muscle cDNAs. As a result, seven of the eight splice variants reported were definitely identified, but we could not identify *ERRγ3* in this study. Although we carefully searched many other human tissues, the mRNA corresponding to *ERRγ3* was not detected. Instead, we identified another novel variant *ERRγ2-bcd* (accession number AB362218). It should be noted that these variants have variable nucleotide sequences of the 5′-UTR, with no structural changes of ERRγ2 protein.

We now know nine splicing variants in total. It should be noted, however, that these variants afford or produce three distinctly different protein isoforms (Fig. 1), as the variants are classified into three mRNA isoforms: *ERRγ1*, *ERRγ2* and *ERRγ3*. Here, type-2 mRNA *ERRγ2* consists of seven subclasses of splicing variants: *ERRγ2-df*, *ERRγ2-def*, *ERRγ2-di*, *ERRγ2-d*, *ERRγ2-ad*, *ERRγ2-bcd* and *ERRγ2-gig* (Fig. 1C), although all of these variants produce the same receptor protein molecule of ERRγ2. The variants are constituted from 15 distinct exons, A–O, coded in the human genomic DNA in the very broad region of chromosome 1 (about 1,000 kbp) (Fig. 1B). The heterogeneity at the 5′-UTR is due to the presence of alternative transcription start sites and alternative splicing sites.

The type-1 protein isoform ERRγ1 has an additional 23-mer elongated N-terminal sequence. Type-2 mRNA genes, *ERRγ2* isoforms, include six variants containing the exon D-based fragment (designated *d*) in the 5′UTR. *ERRγ2-ad*, where *ad* indicates that the exons *a* and *d* are involved in this order, was first isolated from the human fetal brain library by Eudy *et al.* (*13*). On the other hand, *ERRγ2-gig* has been found only in the skeletal muscle cDNA library (*14*). The mRNA *ERRγ3-bcf* gene producing ERRγ3 has recently been reported by Kojo *et al.* (*15*), although we could not identify this gene in the present study. The ERRγ3 protein isoform has a deletion of 39-mer amino-acid residues in the DNA-binding domain of ERRγ2, resulting in an incomplete construction of the DNA binding site. In addition, it was found that *ERRγ* mRNAs each have two alternative polyadenylation isoforms (*13*).

Quantitative Analysis of ERRγ mRNA Genes as a Whole by Real-Time PCR—By means of real-time PCR, the total expression amount of the human *ERRγ* mRNA genes was estimated to amplify the region common to all the splicing variants. We designated the *hERRγ-whole* mRNA segment. We did confirm that there is no contamination of the genomic DNA in these RNA samples, since we could not amplify any cDNA when we used the primer sets directly for the samples.

To analyse the *hERRγ-whole* mRNA gene by real-time PCR, the primer set of sense hERRγwholeF and antisense hERRγwholeR was utilized (Table 2). For the quantification of each *ERRγ* splicing variant, real-time PCR was carried out by using a series of primer sets

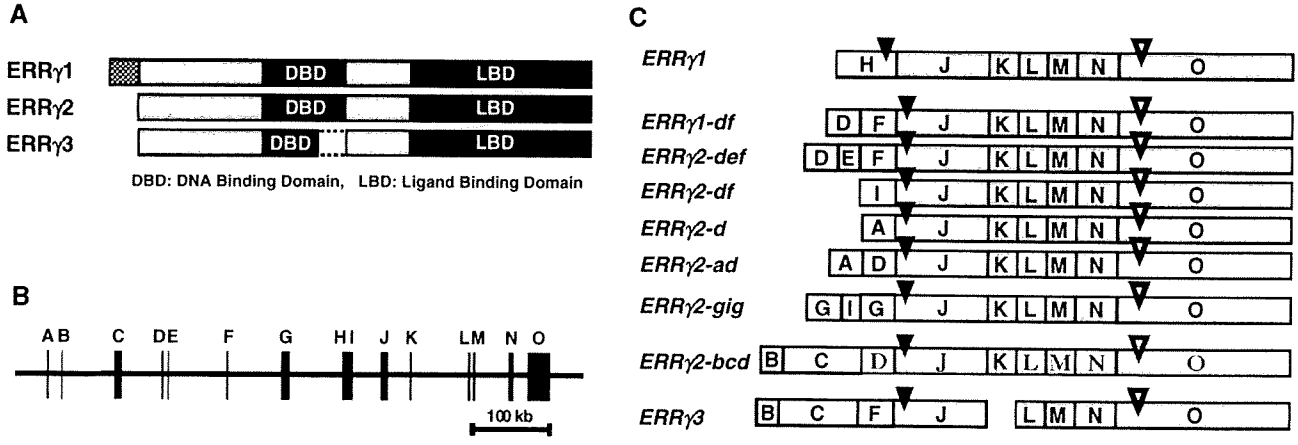

Fig. 1. **Structural constitution of *ERRγ* mRNA isoforms and ERRγ protein isoforms.** (A) Structure of ERRγ protein isoforms. ERRγ1 has 23-mer amino-acid extension at the N-terminus of ordinary ERRγ, namely ERRγ2. ERRγ3 has a 39-mer amino-acid deletion in the DNA binding domain. (B) Structural constitution of exon and intron of human *ERRγ* genomic gene. Alphabetic letters A–O each indicate an independent exon. (C) Structural constitution of exons in nine *ERRγ* mRNA isoforms. Closed arrowheads indicate the position of an AUG initiation codon, and open arrowheads indicate the position of a termination codon in the ERRγ open reading frame.

Table 2. **The nucleotide sequences of the primers used for the quantification of whole ERRγ mRNA and each ERRγ mRNA isoform.**

Name of primers	Oligonucleotide sequences	Length of products (bp)
Primers for quantification of ERRγ-whole mRNA		
hERRγwholeF	5′-CAGAATGTCAAACAAAGATCGACAC-3′	148
hERRγwholeR[a]	5′-GGTTGAACTGTAGCTCCCACTG-3′	
Primers for quantification of ERRγ1 mRNA		
hERRγ1F	5′-GCACATGGATTCGGTAGAACTTTG-3′	215
hERRγ1R[a]	5′-GGTTGAACTGTAGCTCCCACTG-3′	
Primers for quantification of ERRγ2 mRNA		
hERRγ2F	5′-TACGCTAACACTGTCGCAGTTTG-3′	183, 300, 338, 359[b]
hERRγ2R[a]	5′-GGTTGAACTGTAGCTCCCACTG-3′	
Primers for quantification of ERRγ2-gig mRNA		
hERRγ2-gigF	5′-GCCACCACATCTCGATTCAAAG-3′	339
hERRγ2-gigR[a]	5′-GGTTGAACTGTAGCTCCCACTG-3′	
Primers for quantification of ERRγ2-bcd Mrna		
hERRγ2-bcdF	5′-GATGTTGCTACACGGTCCTTCAC-3′	208
hERRγ2-bcdR	5′-TGATCTTCTGCAAAGACCCTACTTC-3′	
Primers for quantification of gapdh mRNA		
hgapdhF	5′-CAGCAAGAGCACAAGAGGAAGA-3′	107
hgapdhR	5′-GTCTACATGGCAACTGTGAGGAG-3′	

[a]These antisense primers have the same nucleotide sequence. [b]The number of products depends on the number of alternative splicing sites in the particular region amplified.

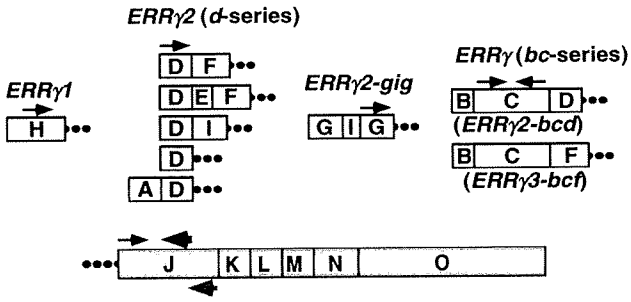

Fig. 2. **Design strategy of forward sense and reverse antisense primers for real-time PCR quantification of *ERRγ* mRNA isoforms.** Rightwards arrows indicate the forward sense primers, while leftwards arrows indicate the reverse antisense primers. Sense primers are specific to each mRNA isoform. For *ERRγ2* containing exon D, *ERRγ2-df*, *def*, *di*, *d*, *ad* and *bcd* the same sense primer was set in exon D (Table 2). For *ERRγ2-bcd* isoforms, sense and antisense primers were set in the same exon, C. There are two different reverse antisense primers in exon J, besides the antisense primer in exon C for *ERRγ2-bcd* isoforms. The large black leftward arrow is a universal antisense primer for the quantification of all isoforms except for *ERRγ2-bcd*. The large grey leftward arrow is an *ERRγ*-specific antisense oligonucleotide for the reverse transcription to prepare cDNAs.

(Fig. 2, Table 2). These primers were designed not to amplify the *ERRγ* sequence on the genomic DNA, setting both sense and antisense primers in the independent exon region.

Real-time PCR was carried out at least three times for the cDNAs prepared from each total RNA sample of human adult kidney, placenta, ovary, uterus, prostate, testis and brain, as well as from the human fetal brain. We determined the number of molecules of the whole mRNA and respective mRNA isoforms, with 1×10^5 molecules of *gapdh* mRNA being the internal standard. For example, the molecular number of the *hERRγ-whole* mRNA of adult brain was 942 per 1×10^5 *gapdh* mRNA (Table 3). The fetal brain had 739 molecules (about 80% of the molecular number of adult brain).

In kidney, *hERRγ-whole* mRNA had a molecular number of 4,369, approximately 4.6-fold that of the adult brain (Table 3). Among the reproductive organ tissues, the placenta was found to express the highest number of *hERRγ-whole* mRNA molecule, 4,544, ~5% greater than that of kidney and thus about 5-fold that of the adult brain. This very high expression of *hERRγ* mRNA genes in the placenta was of course found to exceed those of other reproductive organs: 151 in ovary, 167 in uterus and 571 in testis (Fig. 3). The second highest amount was in the prostate (*1,637*) (Table 3). Thus, the amount in the placenta was approximately 3-fold greater than that in the prostate. These results suggest that ERRγ plays a very significant role in the placental functions. This may indicate adversely that the placenta is potentially the most affected by BPA.

Tissue Distribution Analysis of ERRγ mRNA Splicing Variants by Real-Time PCR—After real-time PCR to measure the *ERRγ-whole* mRNAs, we measured the ratio of each *ERRγ* mRNA isoform—*ERRγ1*, *ERRγ2*, *ERRγ2-gig* and *ERRγ3*—in the tissues. The amount of *ERRγ2-gig* needs to be estimated separately, because the forward sense primer specific for *ERRγ2-gig* is different from that for other *d*-containing *ERRγ2* isoforms. The approximate ratio of each mRNA isoform was calculated against the total number of copies of all mRNA isoforms. As a result, we could calculate the ratio of each *ERRγ* mRNA isoform among the total amount of *ERRγ-whole* mRNA (Table 3 and Fig. 4). Detailed data for these analyses are shown in the Table 4, in which donor

Table 3. **The results of real-time PCR quantification of *ERRγ-whole* mRNA and its subtypes in human tissues.**

Tissues	*ERRγ-whole* mRNA[a]	*ERRγ* mRNA isoforms (%)			
		Type-1	Type-2		
			d-series	*gig*	*bcd*[b]
Brain (adult)	942 ± 24	26.1 ± 9.5	73.5 ± 9.8	0.3 ± 0.2	0.1 ± 0.1
Brain (fetal)	739 ± 195	30.2 ± 11.6	68.8 ± 11.1	0.8 ± 0.6	0.2 ± 0.2
Kidney	4369 ± 1276	11.1 ± 2.8	88.4 ± 3.1	0.3 ± 0.2	0.2 ± 0.1
Pancreas	2742 ± 798	4.0 ± 0.3	94.7 ± 1.2	0.7 ± 0.7	0.6 ± 0.5
Skeletal muscle	247 ± 48	45.2 ± 18.3	7.1 ± 1.0	47.7 ± 18.1	0.0 ± 0.0
Placenta	4544 ± 1572	98.9 ± 0.7	1.1 ± 0.7	0.0 ± 0.0	0.0 ± 0.0
Prostate	1637 ± 217	20.2 ± 2.7	78.2 ± 3.4	1.4 ± 0.6	0.2 ± 0.2
Testis	571 ± 93	23.6 ± 1.9	63.8 ± 1.6	11.0 ± 0.4	1.6 ± 1.1
Ovary	151 ± 50	18.0 ± 4.1	76.2 ± 8.1	3.5 ± 3.5	2.3 ± 2.2
Uterus	167 ± 127	4.3 ± 2.3	93.1 ± 3.7	2.6 ± 2.6	0.0 ± 0.0

[a]The amount of mRNA was calculated as the number of molecules per 1.0×10^5 *gapdh* mRNA molecules. [b]The analysis with specific sense and antisense primers, both of which were set in the same exon C (Fig. 2) was originally designed to measure the total amount of *c*-containing *ERR* mRNAs including *ERRγ2-bcd* and *ERRγ3-bcf*. Since the amount of *ERRγ3-bcf* that gives ERRγ3 was negligible, the measurement gave the amount of only *ERRγ2-bcd* that affords ERRγ2.

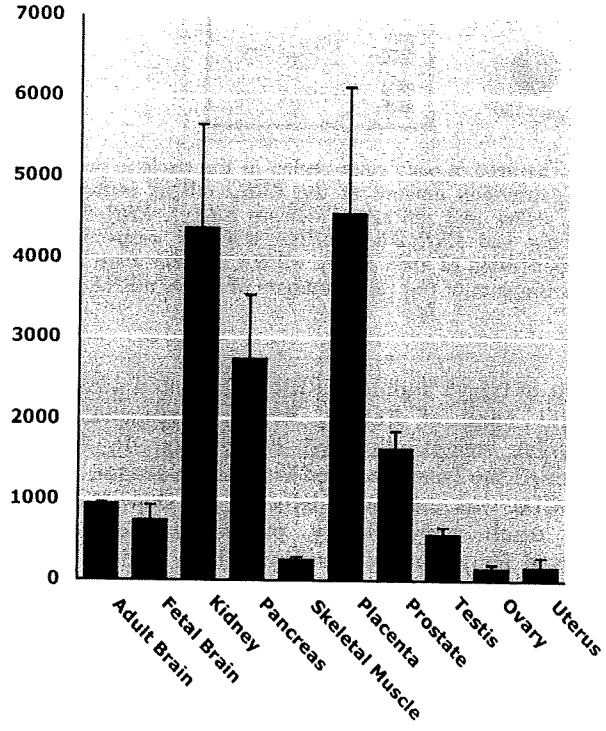

Fig. 3. **Quantitative real-time PCR for estimation of *ERRγ* mRNA expression in human brains and reproductive organs.** The *gapdh* mRNA gene was used as an internal control. The copy number per 1×10^5 *gapdh* mRNA was estimated for *ERRγ-whole* mRNA in each tissue. The error bars indicate SEM.

information such as age and sex is given for samples provided from each agent.

It should be noted that in the placenta, the *ERRγ1* mRNA isoform is accounted for 98.9% of the quantity of all mRNA isoforms (Table 3). This predominance of the type-1 mRNA isoform is very surprising and unique among the human tissues. All other human tissues express *ERRγ2* as a major mRNA isoform. It is likely that ERRγ1 produced from the *ERRγ1* mRNA isoform may play a crucial and central role in the placenta.

Reproductive tissues other than placenta expressed the *ERRγ2* mRNA isoform much more than *ERRγ1*. The content of *ERRγ2* mRNA isoform was estimated as 79.6% in prostate, and 81.9% and 95.7% in ovary and uterus, respectively (Table 3). Since the expression level of *ERRγ2-gig* mRNA was almost negligible in these tissues (Table 4), estimated *ERRγ2* mRNA isoform includes exclusively six subclasses of splicing variants (*d*-series that contain: *ERRγ2-df*, *ERRγ2-def*, *ERRγ2-di*, *ERRγ2-d*, *ERRγ2-ad* and *ERRγ2-bcd*) (Fig. 1C). As for the testis, however, a prominent inconsistency was found. It contained about 11% of the *ERRγ2-gig* mRNA isoform. Furthermore, a discrepancy between the sum of all mRNA isoforms and the *ERRγ-whole* mRNA—the sum of total numbers of *ERRγ* mRNA isoform molecules was clearly smaller (by about 10%) than the total molecular number of *ERRγ-whole* mRNA (data not shown)—strongly suggested the presence of mRNA isoform(s) other than those measured.

The adult and fetal brains were found to have almost the same isoform constitutions (Table 3). The expression ratios of *ERRγ1* and *ERRγ2* mRNAs respectively were 30.2% and 69.8% in the fetal brain and 26.1% and 73.9% in the adult brain. Thus, brain is the tissue in which type-2 *ERRγ* mRNA is expressed predominantly. In kidney, the expression levels of *ERRγ1* and *ERRγ2* mRNAs were estimated to be approximately 11.1% and 88.9%, respectively. Pancreas was also one of the tissues in which type-2 *ERRγ* mRNA was expressed predominantly, 4.0% *ERRγ1* and 96.0% *ERRγ2*. The sum of *ERRγ1* and *ERRγ2* mRNAs occupied approximately 100% in these tissues.

The constitutional ratio of *ERRγ1*, *ERRγ2*(*d*-series) and *ERRγ2-gig* mRNAs in skeletal muscle was unique (Table 3). Their expression ratios were 45.2%, 7.1% and 47.7%, respectively. Skeletal muscle was found to be the tissue in which type-2 *ERRγ2-gig* mRNA is expressed very highly.

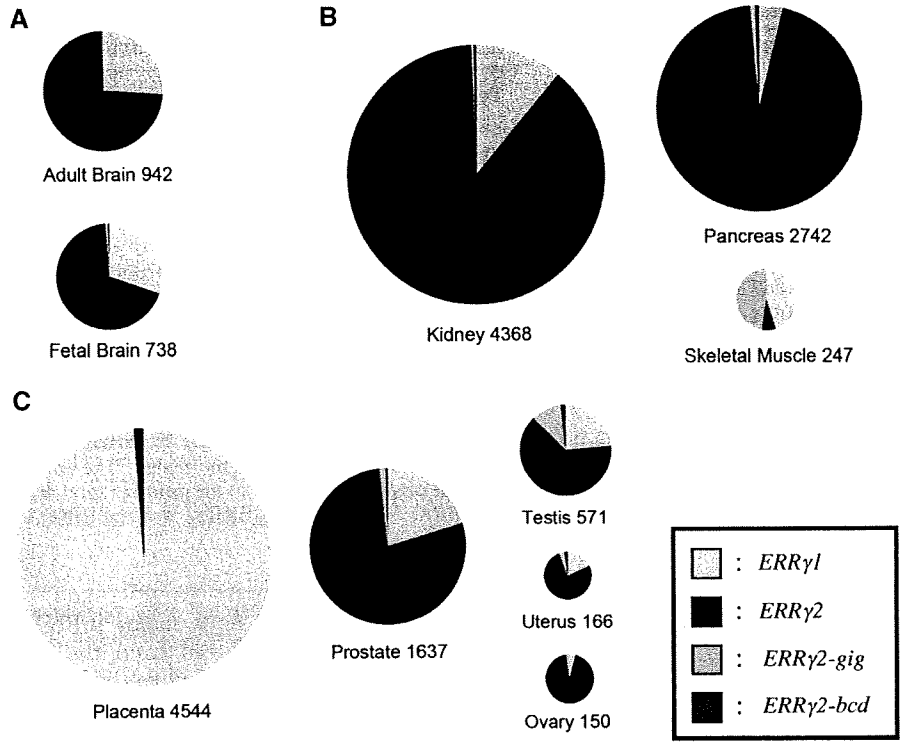

Fig. 4. **Quantitative real-time PCR for estimation of *ERRγ-whole* mRNA expression and percentage of the constitutions of *ERRγ* mRNA isoforms in human brains (A), standard tissues (kidney, pancreas and skeletal muscle) (B) and reproductive organs (C).** The circled area shows the total expression amount of *ERRγ-whole* mRNA in each tissue. The area of each color region in the circle is proportional to the expression amount of the *ERRγ* mRNA isoforms. Blue, purple, yellow and red areas indicate *ERRγ1*, *ERRγ2*(*d*-series), *ERRγ2-gig* and *ERRγ2-bcd* mRNA isoforms, respectively. The expression rates of each *ERRγ* mRNA isoform were calculated against the sum of the copy numbers of *ERRγ* mRNA isoforms.

In the estimation of the tissue distributions of *ERRγ* mRNA splicing variants, another important issue is to calculate the actual amount of each mRNA isoform. As shown in Fig. 4, *ERRγ1* mRNA isoform was most abundant in placenta, the amount of this isoform ($4{,}544 \times 98.9\%$ as in Table 3 = 4,494 molecules) being exclusive and predominant. The kidney is the tissue in which the *ERRγ2* mRNA isoform is richest (3,884). Pancreas (2,632) and prostate (1,306) are also abounding in *ERRγ2*. As for the *ERRγ2-gig* mRNA isoform, skeletal muscle (118) and testis (63) contain it relatively highly.

Western Blotting Detection of ERRγ Protein Isoforms—To verify the amount of type-1 ERRγ protein isoform expressed in the placenta, Western blotting was carried out for the lysates of the human placenta and kidney. Kidney was selected as a reference because of its expected high expression (~90%) of the type-2 ERRγ protein isoform (see above). ERRγ protein isoforms were detected by using a monoclonal antibody specific for the N-terminal region (1–100) of ERRγ2, because this antibody can detect all three isoforms: ERRγ1, ERRγ2 and ERRγ3. The calculated molecular weight (51,313) of type-1 ERRγ is larger than that of type-2 standard ERRγ by ~2,700, apparently due to the N-terminal addition of 23-mer amino-acid residues.

The lysate isolated from kidney exhibited an intense protein band of 49 kDa, corresponding to the molecular weight of type-2 standard ERRγ. This band accompanied a faint band of 51 kDa, which corresponds to the molecular weight of type-1 ERRγ (Fig. 5). When we examined the lysate isolated from the placenta, the band of 51 kDa was markedly detected, as shown in Fig. 5. This result very clearly proves the consequences observed for the mRNA isoforms. It is evident that the mRNA variants expressed indeed produce a consequent protein and that the placenta expresses the type-1 ERRγ protein isoform predominantly and exclusively.

Transcription Activity of Type-1 and Type-2 ERRγ Isoforms in the Reporter Gene Assay—ERRγ is a constitutively active nuclear receptor that exhibits a high basal activity with no ligand. In the present study, we examined the reporter gene activity of type-1 and type-2 ERRγ isoforms by means of the luciferase reporter gene assay using HeLa cells. To normalize for transfection efficiency, we simultaneously carried out the SEAP assay (*16*). When the type-1 ERRγ isoform was compared with the type-2 standard ERRγ isoform, the constitutive activity level of type-1 ERRγ was found to be about 50% higher than that of type-2 ERRγ. As shown in Fig. 6, the type-2 ERRγ isoform exhibited significantly elevated constitutive activity (210% of the basal activity). Type-1 ERRγ isoform also exhibited considerably elevated constitutive activity (260%), a notably higher level than that of type-2. The results indicate that the N-terminal

Table 4. **Donor information for quantification of ERRγ-whole mRNA and its subtypes by quantitative real-time PCR.**

Tissues	Agent sources[a]	Age	Sex[b]	Number of donors	*ERRγ- whole* mRNA[c]	*ERRγ* mRNA isoforms (%)[d]			
						Type-1	Type-2		
							d-series	*gig*	*bcd*[e]
Brain	C	47–55	M	2	933	45.0	54.0	0.7	0.3
(adult)	S	66	F	1	906	18.1	81.9	0.0	0.0
	B	30	M	1	988	15.2	84.7	0.1	0.0
Brain	C	26–40[f]	M/F	21	555	15.5	82.1	1.9	0.5
(fetal)	S	19[f]	M	1	1128	53.2	46.8	0.0	0.0
	B	28[f]	F	1	533	21.9	77.4	0.6	0.1
Kidney	C	18–59	M/F	14	2540	16.5	82.4	0.7	0.4
	S	67	F	1	3742	7.2	92.7	0.0	0.1
	B	24	M	1	6824	9.7	90.2	0.0	0.1
Pancreas	C	35	M	1	4024	3.8	92.4	2.2	1.6
	S	72	M	1	1278	3.5	96.5	0.0	0.0
	B	44	M	1	2925	4.6	95.3	0.0	0.1
Skeletal	C	20–68	M/F	7	152	18.1	8.7	73.1	0.1
muscle	S	85	F	1	307	80.0	7.3	12.7	0.0
	B	87	F	1	283	37.3	5.4	57.3	0.0
Placenta	C	21–33	F	16	7538	99.6	0.3	0.1	0.0
	S	28	F	1	3880	99.5	0.5	0.0	0.0
	B	26	F	1	2214	97.6	2.4	0.0	0.0
Prostate	C	21–50	M	32	1420	22.8	74.8	2.0	0.4
	B	69	M	1	1854	17.5	81.6	0.9	0.0
Testis	C	24–64	M	39	693	21.7	62.9	11.7	3.7
	S	72	M	1	389	21.8	66.9	10.3	1.0
	B	27	M	1	632	27.3	61.7	11.0	0.0
Ovary	C	20–60	F	15	70	20.8	61.9	10.6	6.7
	S	49	F	1	139	10.0	90.0	0.0	0.0
	B	46	F	1	243	23.2	76.8	0.0	0.0
Uterus	C	40–61	F	3	70	4.9	87.3	7.8	0.0
	S	88	F	1	419	8.0	91.9	0.0	0.1
	B	49	F	1	11	0.0	100	0.0	0.0

[a]The samples of total RNA extracted from human tissues were purchased from Clontech (C), Stratagene (S) and BioChain (B). [b]M and F represent male and female, respectively. [c]The amount of mRNA was calculated as the number of molecules per 1.0×10^5 *gapdh* mRNA molecules. [d]The same antisense primer for *hERRγ-whole* mRNA was utilized for the quantification of *ERRγ1* and *ERRγ2* (Table 2). [e]The real-time PCR quantification to measure *c*-containing *ERR* mRNAs was carried out. Since the amount of *ERRγ3-bcf* was negligible, this counting was found to be just for *ERRγ2-bcd* that affords ERRγ2. [f]The age of fetal brain is shown by the number of weeks.

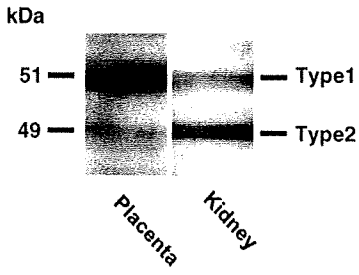

Fig. 5. **Western blotting analyses of ERRγ protein isoform expression levels.** An intense protein band of 49 kDa in kidney lysate corresponds to the molecular weight of type-2 standard ERRγ. The accompanying faint band of 51 kDa corresponds to the molecular weight of type-1 ERRγ. A major strong band of 51 kDa in the placenta lysate corresponds also to this type-1 ERRγ. Other bands are supposed to be specific or non-specific protein bands derived from the first antibody.

23-mer elongation has a distinct effect on the reporter gene transactivation activity of ERRγ.

4-OHT deactivated the ordinary standard type-2 ERRγ, as reported (*7*, *17*), diminishing the basal activity of ERRγ by up to 60–80% at a concentration of 10 μM (Fig. 7A). These were exactly revealed for the type-1 ERRγ isoform, ERRγ1. BPA, on the other hand, showed no effect on the basal constitutive activity of ERRγ even at a concentration of 10 μM, completely preserving ERRγ's high constitutive activity (Fig. 7A). The inverse agonist activity of 4-OHT for ERRγ1 was reversed or inhibited by BPA in a dose-dependent manner (Fig 7B). This reversing activity of BPA, namely, inverse antagonist activity of BPA, was revealed originally for the type-2 ERRγ isoform (*7*).

DISCUSSION

Extremely High Expression of ERRγ *mRNA in the Placenta*—In the present study, using commercially available human gene samples of reproductive organ

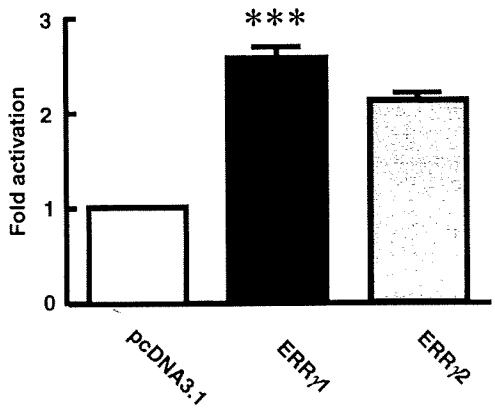

Fig. 6. **Transcription activity of type-1 and type-2 ERRγ isoforms in the reporter gene assay.** The type-1 ERRγ isoform is 23-mer larger than the type-2 ordinary ERRγ isoform at the N-terminus. HeLa cells were transfected with the luciferase reporter gene (3 × ERRE) and the expression plasmid of the wild-type of either type-1 or type-2 ERRγ. After 24 h, luciferase activity was measured. Cells treated with 1% BSA/PBS were used as a vehicle control. Each assay was performed in duplicate and repeated at least three times. To normalize the transfection efficiency, the SEAP assay, in which a second plasmid that constitutively expresses an activity that can be clearly differentiated from SEAP, was co-transfected simultaneously. (***$P < 0.0001$: ANOVA)

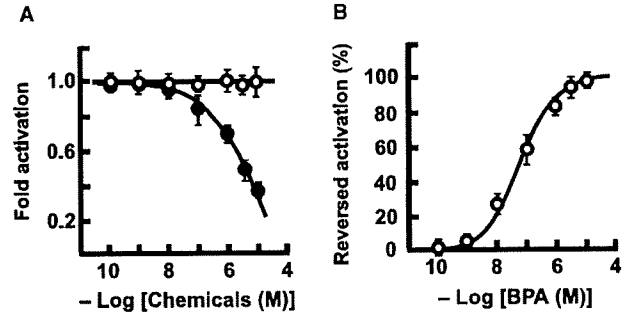

Fig. 7. **The luciferase reporter gene assay of BPA and 4-hydroxytamoxifen (4-OHT) for type-1 ERRγ.** (A) Deactivation of the fully activated human type-1 ERRγ isoform by the *inverse agonist* 4-hydroxytamoxifen (4-OHT) (filled circle) and sustainment by the *inverse antagonist* BPA (open circle). (B) Inverse antagonist activity of BPA (open circle) against the inverse agonist activity of 1.0 μM 4-OHT in ERRγ1. An amount of 1.0 μM 4-OHT exhibited ~0.4-fold deactivation, and the inverse antagonist activities are shown by the percentage of relative activity to reverse this deactivation activity. The high basal constitutive activity of type-1 ERRγ isoform was evaluated with the luciferase reporter plasmid (pGL3/3 × ERRE), and the highest activity was estimated in a cell preparation of 1.0×10^5 HeLa cells/well.

tissues and brains, we succeeded in the tissue distribution analyses of the *ERRγ-whole* mRNA gene and the constitutional ratios of a series of *ERRγ* mRNA isoforms. Real-time PCR for *whole-ERRγ* mRNA demonstrated an unexpectedly high expression of *ERRγ* mRNA in the placenta (Fig. 3). Western blotting also confirmed the expression of ERRγ protein (Fig. 5).

For accuracy in the quantification of *hERRγ-whole* mRNA, we repeated the real-time PCR. By using a new set of sense and antisense primers set at the 3′ terminal region, the results eventually obtained were almost the same as those of the first quantification shown in Fig. 3 (data not shown). For further confirmation, we tested internal controls other than *gapdh* mRNA. Those include the mRNA genes of human *β-actin*, *ubiquitin C*, *sdha* (succinate dehydrogenase complex, subunit A) and *hprt1* (hypoxanthine phosphoribosyl-transferase I). The results for the amount of *ERRγ* mRNA were almost the same as those obtained by the quantification using *gapdh* mRNA (data not shown). These further evidenced that the *ERRγ* mRNA expression in the human placenta is extreme, and the highest among the tissues examined.

Other reproductive organ tissues, such as ovary, uterus and testis, also express *ERRγ* mRNA, but at very low levels: 3.3%, 3.7% and 12.6% that of the placenta, respectively. Compared to these tissues, the considerably high expression of *ERRγ* mRNA in the prostate should be noted. The prostate had the second highest amount of *ERRγ* mRNA, approximately 36% of that in the placenta.

Predominant Expression of Type-1 Isoform of ERRγ *mRNA in the Placenta*—Nuclear receptors usually have several mRNA and protein isoforms by alternative splicing mechanisms, resulting in the exhibition of their functions in a tissue-specific or developmental stage-specific manner (*10*, *11*). Unfortunately, there is little understanding not only of the physiological functions of splicing variants, especially *in vivo*, but also of their tissue distributions in the majority of tissues throughout the body.

All transcript *ERRγ* mRNA variants consist of several distinct exons coded on human genomic DNA in the very broad region of chromosome 1 (about 1,000 kbp). As shown in Fig. 1B, the exons are thought to be distinguished between those in a variable region (A~I) and those in a consistent region (J~O). The latter includes almost all of the open reading frames of ERRγ, while 1–3 exons are selected from the variable region to form a 5′-UTR. Including alternative polyadenylation mechanisms, the gene expression of ERRγ appears to be severely regulated in a post-transcriptional manner. The sequence difference of the 5′-UTR should bring about a different translational efficiency, depending on the stability of mRNA produced and the presence of some upstream open reading frames (uORF) (*18*).

Type-1 ERRγ isoform (ERRγ1) has an additional 23-mer amino-acid residue extension at the N-terminus, and exhibits about 50% increased basal constitutive activity relative to that of ERRγ2 (Fig. 6). Although this isoform possesses exactly the same structure of its ligand-binding domain as other isoform types, its activation mechanism may differ from those of other isoforms by having this 23-mer N-terminal elongation. This might bring about unique tissue-specific function(s) in the placenta.

High Concentration of BPA in the Placenta due to High Expression of Type-1 ERRγ—BPA is an industrial chemical, and exposure to it is now widespread (*19*, *20*). We know now that BPA binds to ERRγ about 100 times greater than to ERα and ERβ, and that BPA exhibits a distinct inhibition activity against 4-OHT in ERRγ.

In the present study, we did know that there are three isoforms possessing precisely the same ligand-binding domain (LBD). It should be noted that BPA can bind to all these ERRγ isoforms in any tissue.

This strongly suggests that the concentration of BPA in human tissues is directly proportional to the amount of ERRγ proteins. In our estimation in the present study involving reproductive organ tissues, the expression of *ERRγ* mRNA is largest in the placenta and second largest in the prostate. The BPA concentration in the placenta has been reported to be approximately five times higher than that in maternal and fetal plasma (*21*). It is now quite reasonable to believe that the high concentration of BPA is due to the large amount of ERRγ protein isoforms, almost entirely type 1, in the human placenta.

The Effects of BPA Accumulation or Binding to Type-1 ERRγ on Placental Functions—The placenta receives nutrients, oxygen, antibodies and hormones from the mother's blood and removes waste. It forms the placental barrier, which filters out some substances that could harm the fetus. However, some substances, including BPA and viruses, are not filtered out, suggesting that the placenta does not act as a barrier against BPA (*21*, *22*). In addition to transferring gases and nutrients, the placenta also has metabolic and endocrine activity. It produces estrogen, relaxin, and human chorionic gonadotrophin, progesterone and somatomammotropin, all of which are important in maintaining pregnancy and the large amounts of glucose and lipids in the maternal blood. It is now evident that the placenta expresses BPA receptor ERRγ very highly. What would happen with the accumulation of BPA in the placenta?

Placentation in BPA-administered mice during pregnancy was reported to be abnormal (*23*), directly decreasing the number of embryos. In addition, almost all mouse neonates exposed to BPA were dead within 3 days after birth. Thus, BPA might disrupt the placental functions directly or indirectly, and might affect the mortality of neonates through indirect exposure of embryos. These are likely mediated through the BPA receptor ERRγs, at least in part. BPA administration has also been reported to significantly increase the weight of the uterus and the number and fertilization quality of sperm (*24*). DNA microarray analysis has shown that BPA administration increases the mRNAs of some nuclear receptors in mouse placenta (*25*). These results suggest that BPA affects the transcriptional regulation in the placenta or other reproductive organs through certain particular transcription factors.

Based on the fact that BPA strongly binds to ERRγ, the abnormality and probable change of gene expression in the placenta are likely accompanied by BPA binding to ERRγ. In this study, we demonstrated that the *ERRγ1* mRNA gene expresses almost fully in the placenta, and that the resulting type-1 ERRγ receptor is noticeably more potent than the resulting type-2 ERRγ receptor that expresses dominantly in other tissues. BPA would sustain unnecessarily this very high basal constitutional activity of type-1 ERRγ receptor in the placenta.

Other Human Tissues with High Expression of ERRγ *mRNA*—Adult and fetal brains, kidney and pancreas were the tissues in which ERRγ expresses significantly and considerably highly. In these tissues, type-2 *ERRγ* mRNA is expressed predominantly, while the expression levels of *ERRγ3* is almost negligible. The expression ratios of *ERRγ1* and *ERRγ2* mRNAs respectively varied 4–30% and 69–95%. As compared to the type-2 ERRγ isoform (ERRγ2), type-1 isoform ERRγ1 has an additional 23-mer amino-acid elongation at the N-terminus. Although ERRγ1 exhibits about 50% increased basal constitutive activity relative to that of ERRγ2 (see above), physiological functions in these tissues have never been clarified nor analysed for both ERRγ1 and ERRγ2.

As for the prostate, the mRNA gene was for the most part (~80%) *ERRγ2*. Various effects of estrogenic chemicals including BPA have been reported for the prostate. For example, acceleration in the proliferation rate of prostate epithelium during fetal life was noted to disrupt permanently the cellular control systems and to predispose the prostate to disease in adulthood (*26*, *27*). The effects of estrogens on the prostate, or the effects of their involvement in prostate cancer development and benign prostatic hyperplasia, are likely mediated through their ERs. In addition to the androgen receptor, which plays a central role in the normal development and neoplastic growth of the prostate gland, estrogens have long been suggested to play synergetic or distinct roles in the same processes. However, studies from ER knockout mouse models have shown neither ERα nor ERβ affects the targeted disruption of prostatic phenotype and function (*28*). This strongly suggests the involvement of one or more nuclear receptors other than ER and that ERRγ is a probable candidate for involvement in prostatic growth and development. ERRγ might play regulatory roles in normal and neoplastic prostatic cells by sharing similar ER-mediated pathways or acting independently.

CONCLUSION

The present study provides a valuable blueprint of ERRγ mRNA expression and important clues to understanding BPA's low-dose effects in humans. For instance, although the issue of bioavailability of parent BPA in humans has been contentious, the present results strongly suggest that the BPA concentration is proportional to the expression amount of ERRγ. There are scientific debates over whether or not low doses of BPA can have developmental or reproductive effects in humans. Now, it is clear that ERRγ, the receptor of BPA, abounds in brains and reproductive tissues such as the placenta and prostate.

Strong expression of ERRγ as a possible receptor of BPA in both the placenta and the fetal brain could have important implications for newborns. ERRγ is also a probable candidate for involvement in prostatic growth and development. However, the physiological roles of ERRγ are poorly understood at the moment. It is thus important to clarify such physiological functions and characteristics of ERRγ. Moreover, it is crucial to examine the content and extent of which BPA may influence these roles.

FUNDING

Health and Labour Sciences Research Grants for Research on the Risk of Chemical Substances, from the Ministry of Health, Labor and Welfare of Japan (to Y.S.); grants-in-aid from the Ministry of Education, Culture, Sports, Science and Technology of Japan (to Y.S.).

CONFLICT OF INTEREST

None declared.

REFERENCES

1. Krishnan, A.V., Stathis, P, Permuth, S.F., Tokes, L., and Feldman, D. (1993) Bisphenol-A: an estrogenic substance is released from polycarbonate flasks during autoclaving. *Endocrinology* **132**, 2279–2286
2. Olea, N., Pulgar, R., Perez, P., Olea-Serrano, F., Rivas, A., Novillo-Fertrell, A., Pedraza, V., Soto, A.M., and Sonnenschein, C. (1996) Estrogenicity of resin-based composites and sealants used in dentistry. *Environ. Health Perspect.* **104**, 298–305
3. Sohoni, P. and Sumpter, J.P. (1998) Several environmental oestrogens are also anti-androgens. *J. Endocrinol.* **158**, 327–339
4. Xu, L.C., Sun, H., Chen, J.F., Bian, Q., Qian, J, Song, L, and Wang, X.R. (2005) Evaluation of androgen receptor transcriptional activities of bisphenol A, octylphenol and nonylphenol *in vitro*. *Toxicology* **216**, 197–203
5. Okada, H., Tokunaga, T., Liu, X., Takayanagi, S., Matsushima, A., and Shimohigashi, Y. (2008) Direct evidence revealing structural elements essential for the high binding ability of bisphenol A to human estrogen-related receptor-γ. *Environ. Health Perspect.* **116**, 32–38
6. Liu, X., Matsushima, A., Okada, H., Tokunaga, T., Isozaki, K., and Shimohigashi, Y. (2007) Receptor binding characteristic of the endocrine disruptor bisphenol A for the human nuclear estrogen-related receptor γ. Chief and corroborative hydrogen bonds of the bisphenol A phenol-hydroxyl group with Arg316 and Glu275 residues. *FEBS J.* **274**, 6340–6351
7. Takayanagi, S., Tokunaga, T., Liu, X., Okada, H., Matsushima, A., and Shimohigashi, Y. (2006) Endocrine disruptor bisphenol A strongly binds to human estrogen-related receptor γ (ERRγ) with high constitutive activity. *Toxicol. Lett.* **167**, 95–105
8. Matsushima, A., Kakuta, Y., Teramoto, T., Koshiba, T., Liu, X., Okada, H., Tokunaga, T., Kawabata, S., Kimura, M., and Shimohigashi, Y. (2007) Structural evidence for endocrine disruptor bisphenol A binding to human nuclear receptor ERRγ. *J. Biochem.* **142**, 517–524
9. Matsushima, A., Teramoto, T., Okada, H., Liu, X., Tokunaga, T., Kakuta, Y., and Shimohigashi, Y. (2008) ERRγ tethers strongly bisphenol A and 4-α-cumylphenol in an induced-fit manner. *Biochem. Biophys. Res. Commun.* **373**, 408–413
10. Lu, N.Z. and Cidlowski, J.A. (2005) Translational regulatory mechanisms generate N-terminal glucocorticoid receptor isoforms with unique transcriptional target genes. *Mol. Cell* **18**, 331–342
11. Wang, Z., Zhang, X., Shen, P., Loggie, B.W., Chang, Y., and Deuel, T.F. (2006) A variant of estrogen receptor-α, hER-α36: Transduction of estrogen- and antiestrogen-dependent membrane-initiated mitogenic signaling. *Proc. Natl Acad. Sci. USA* **103**, 9063–9068
12. NTP-CERHR Monograph on the potential human reproductive developmental effects of bisphenol A (NIH Publication No. 08–5994; September 2008).
13. Eudy, J.D., Yao, S., Weston, M.D., Ma-Edmonds, M., Talmadge, C.B., Cheng, J.J., Kimberling, W.J., and Sumegi, J. (1998) Isolation of a gene encoding a novel member of the nuclear receptor superfamily from the critical region of Usher syndrom type IIa at 1q41. *Genomics* **50**, 382–384
14. Heard, D.J., Norby, P.L., Holloway, J., and Vissing, H. (2000) Human ERRγ, a third member of the estrogen receptor-related receptor (ERR) subfamily of orphan nuclear receptors: tissue-specific isoforms are expressed during development and in the adult. *Mol. Endocrinol.* **14**, 382–392
15. Kojo, H., Tajima, K., Fukagawa, M., Isogai, T., and Nishimura, S. (2006) A novel estrogen receptor-related protein γ splice variant lacking a DNA binding domain exon modulates transcriptional activity of a moderate range of nuclear receptors. *J. Steroid Biochem. Mol. Biol.* **98**, 181–192
16. Sambrook, J. and Russell, D.W. (2001) *Molecular Cloning: A Laboratory Manual* Cold Spring Harbor Laboratory Press, 3rd edn., Cold Spring Harbor, NY
17. Coward, P., Lee, D., Hull, M.V., and Lehmann, J.M. (2001) 4-Hydroxytamoxifen binds to and deactivates the estrogen-related receptor gamma. *Proc. Natl Acad. Sci. USA* **98**, 8880–8884
18. Meijer, H.A. and Thomas, A.A. (2002) Control of eukaryotic protein synthesis by upstream open reading frames in the 5'-untranslated region of an mRNA. *Biochem. J.* **367**, 1–11
19. vom Saal, F.S. (2006) Bisphenol A eliminates brain and behavior sex dimorphisms in mice: how low can you go? *Endocrinology* **147**, 3679–3680
20. Welshons, W.V., Nagel, S.C., and vom Saal, F.S. (2006) Large effects from small exposures. III. Endocrine mechanisms mediating effects of bisphenol A at levels of human exposure. *Endocrinology* **147**, S56–S69
21. Schonfelder, G., Wittfoht, W., Hopp, H., Talsness, C.E., Paul, M., and Chahoud, I. (2002) Parent bisphenol A accumulation in the human maternal-fetal-placental unit. *Environ. Health Perspect.* **110**, 703–707
22. Takahashi, O. and Oishi, S. (2000) Disposition of orally administered 2,2-bis(4-hydroxyphenyl)propane (bisphenol A) in pregnant rats and the placental transfer to fetuses. *Environ. Health Perspect.* **108**, 931–935
23. Tachibana, T, Wakimoto, Y, Nakamuta, N, Phichitraslip, T, Wakitani, S, Kusakabe, K., Hondo, E., and Kiso, Y. (2007) Effects of bisphenol A (BPA) on placentation and survival of the neonates in mice. *J. Reprod. Dev.* **53**, 509–514
24. Welshons, W.V., Thayer, K.A., Judy, B.M., Taylor, J.A., Curran, E.M., and vom Saal, F.S. (2003) Large effects from small exposures. I. Mechanisms for endocrine-disrupting chemicals with estrogenic activity. *Environ. Health Perspect.* **111**, 994–1006
25. Imanishi, S., Manabe, N., Nishizawa, H., Morita, M., Sugimoto, M., Iwahori, M., and Miyamoto, H. (2003) Effects of oral exposure of bisphenol A on mRNA expression of nuclear receptors in murine placental assessed by DNA microarray. *J. Reprod. Dev.* **49**, 329–336
26. Richter, C.A., Taylor, J.A., Ruhlen, R.L., Welshons, W.V., and vom Saal, F.S. (2007) Estradiol and bisphenol A stimulate androgen receptor and estrogen receptor gene expression in fetal mouse prostate mesenchyme cells. *Environ. Health Perspect.* **115**, 902–908
27. Timms, B.G., Howdeshell, K.L., Barton, L., Bradley, S., Richter, C.A., and vom Saal, F.S. (2005) Estrogenic chemicals in plastic and oral contraceptives disrupt development of the fetal mouse prostate and urethra. *Proc. Natl Acad. Sci. USA* **102**, 7014–7019
28. Jarred, R.A., McPherson, S.J., Bianco, J.J., Couse, J.F., Korach, K.S., and Risbridger, G.P. (2002) Prostate phenotypes in estrogen modulated transgenic mice. *Trends Endocrinol. Metab.* **13**, 163–168

Bioorganic & Medicinal Chemistry 17 (2009) 5683–5687

Contents lists available at ScienceDirect

Bioorganic & Medicinal Chemistry

journal homepage: www.elsevier.com/locate/bmc

Discriminatory synergistic effect of Trp-substitutions in superagonist [(Arg/Lys)^{14}, (Arg/Lys)^{15}]nociceptin on ORL1 receptor binding and activation

Hirokazu Nishimura [a], Jinglan Li [a], Kaname Isozaki [a,†], Kazushi Okada [a,‡], Ayami Matsushima [a], Takeru Nose [a], Tommaso Costa [b], Yasuyuki Shimohigashi [a,*]

[a] Laboratory of Structure-Function Biochemistry, Department of Chemistry, Faculty of Sciences, Kyushu University, Fukuoka 812-8581, Japan
[b] Laboratorio di Farmacologia, Istituto Superiore di Sanità, Viole Regina Elena 299, Roma, Italy

ARTICLE INFO

Article history:
Received 21 April 2009
Revised 3 June 2009
Accepted 5 June 2009
Available online 13 June 2009

Keywords:
Basic amino acids
Antagonist
Nociceptin
Synergistic potentiation
Superagonist

ABSTRACT

ORL1 is an endogenous G protein-coupled receptor for neuropeptide nociceptin. [(R/K)^{14}, (R/K)^{15}]nociceptin is a superagonist that strongly activates the ORL1 receptor. We have previously found that substituting with Trp can reproduce the potentiation induced by Arg or Lys at position 14. In the present study, in order to ensure the effect of Trp-substitution on the activities of [(R/K)^{14}, (R/K)^{15}]nociceptin, we synthesized [W^{14}, (R/K)^{15}]nociceptin and [(R/K)^{14}, W^{15}]nociceptin. [W^{14}, (R/K)^{15}]nociceptin was found to exhibit threefold higher binding activity and 10-fold greater potency in a functional [^{35}S]GTPγS functional assay as compared to wild-type nociceptin. However, when only Trp was placed in position 15, the resulting analogues, [(R/K)^{14}, W^{15}]nociceptin, showed only a moderate enhancement of binding and biological activity (2–3 fold in both). These results indicate that the placement of Trp at position 14, unlike at position 15, enhances in a synergistic fashion the interaction of nociceptin with the ORL1 receptor. The results indicate that specific interactions feasible for Arg/Lys and Trp in common must be there for aromatic residues in ORL1, thus forming a cation/π interaction or π/π hydrophobic interaction. The necessity for a favorable electrostatic interaction appears strict in position 15.

1. Introduction

Nociceptin (Noc),[1,2] FGGFTGARKSARKLANQ, is an endogenous ligand of opioid receptor-like 1 (ORL1) receptor with the seven-transmembrane structure.[3–6] Nociceptin induces hyperalgesia[1], and the Noc/ORL1 ligand–receptor system is also involved in many other physiological functions.[7–9] In structure–activity studies of the Noc/ORL1 ligand–receptor system, major efforts have been focused on the design of Noc antagonists as potentially useful analgesics and anti-neuropathy drugs. In contrast, efforts to design and synthesize highly potent and selective ORL1 agonists have also been made. These agonists are of interest because they may not only be able to facilitate the identification of receptor functional residues but may also could result in the discovery of ligands with enhanced desensitization and internalization of the receptor, thus providing a different kind of antagonistic response.[10,11]

Nociceptin contains two Arg-Lys (RK) dipeptide units at positions 8–9 and 12–13. This basic amino acid region is essential for both receptor recognition and activation,[12,13] interacting with a cluster of acidic amino acids in the second extracellular loop of the ORL1 receptor.[14–16] We have previously found that [RK$^{14-15}$]nociceptin ([RK$^{14-15}$]Noc) is a kind of superagonist exhibiting much more potentiated biological activity than expected based on results regarding its receptor-binding activity.[17] RK$^{14-15}$ is now a useful building unit to obtain Noc analogues with enhanced in vitro and in vivo agonist/antagonist activities.[18–25]

We have recently found that three other Noc analogues, [RR$^{14-15}$]Noc, [KK$^{14-15}$]Noc, and [KR$^{14-15}$]Noc, also act as superagonists. Together with [RK$^{14-15}$]Noc, these analogues were found to more synergistically potentiate ORL1 than [(R/K)^{14}]Noc and [(R/K)^{15}]Noc.[26] Furthermore, it appears possible that the Arg or Lys residue at position 14 is replaceable with Trp in terms of such a synergistic potentiation, but not at position 15.[26]

In the present study, in order to ensure the effect of Trp-substitution on the activities of [(R/K)^{14}, (R/K)^{15}]Noc, we synthesized [WR$^{14-15}$]Noc, [WK$^{14-15}$]Noc, [RW$^{14-15}$]Noc, and [KW$^{14-15}$]Noc. We here report their binding activity and biological potency for ORL1 receptor expressed in COS-7 cells. We postulated that Trp, Arg, and Lys incorporated into Noc at position 14 interact specifically with the aromatic residue of ORL1, forming a π/π hydrophobic interaction for Trp or a cation/π interaction for Arg and Lys.

Abbreviations: BCA, bicinchoninic acid; MALDI-TOF, matrix-assisted laser desorption ionization time-of-flight; Noc, nociceptin; ORL1, opioid receptor-like 1; RP-HPLC, reversed-phase HPLC; TFA, trifluoroacetic acid.

* Corresponding author. Tel./fax: +81 92 642 2584.
E-mail address: shimo@chem.kyushu-univ.jp (Y. Shimohigashi).
† Present address: NIH-NINDS-RBU, Bethesda, MD 20892, USA.
‡ Present address: Mebiopharm Co., Ltd, Research and Development, Sumitomo Akasaka Bldg. 5th Floor, 8-10-24, Akasaka, Minato-ku, Tokyo 107-0052, Japan.

0968-0896/$ - see front matter © 2009 Elsevier Ltd. All rights reserved.
doi:10.1016/j.bmc.2009.06.015

2. Results

2.1. Peptide syntheses

As shown in Table 1, Noc and its analogues, seven in total, were evaluated for their activities against ORL1 receptors in this study. In addition to [RK$^{14-15}$]Noc (**1**),[17] we newly synthesized four Trp-containing analogues—that is, [WR$^{14-15}$]Noc (**2**), [WK$^{14-15}$]Noc (**3**), [RW$^{14-15}$]Noc (**5**), and [KW$^{14-15}$]Noc (**6**). Analogues [W^{14}]Noc (**4**) and [W^{15}]Noc (**7**) had been synthesized previously.[27]

All Noc analogues were synthesized by the Fmoc solid-phase methodology. Peptides were obtained with an average yield of approximately 50% (Table 2). The purity was verified by analytical HPLC, in which all peptides emerged as a single peak. The synthesized peptides, all of which contained 5 basic amino acids (Arg and Lys), were eluted at almost the same retention time (approximately 28.5 min) in this reversed-phase (RP)-HPLC (Table 2). Native Noc having 4 basic amino acids was eluted at 29.8 min, while [RK$^{14-15}$]Noc having 6 basic amino acids was eluted at 25.4 min. The measured mass numbers were coincident with the calculated values (Table 2).

2.2. Trp-substitution of Arg^{14} and Lys^{14} with concrete synergistic activity

In the competitive receptor-binding assay, wild-type Noc showed very potent binding to the rat ORL1 receptor expressed in COS-7 cells. The half-maximal concentration (IC_{50}) for inhibition of the binding of [^{3}H]Noc was calculated to be 0.73 nM (Table 3). In the same competitive receptor-binding assay, [RK$^{14-15}$]Noc (**1**) was very potent (IC_{50}, 0.21 nM), displaying a 3.5-fold enhancement of binding activity compared to wild-type Noc (Table 3). The biological activity of wild-type Noc was assessed in the [^{35}S]GTPγS binding assay using membranes prepared from COS-7 cells expressing rat ORL1 receptor. The concentration of wild-type Noc inducing 50% of the maximal stimulation (EC_{50}) was estimated to be 13 nM (Table 4). [RK$^{14-15}$]Noc **1** was the most potent (EC_{50}, 1.1 nM) in this GTPγS functional assay, being approximately 12-fold more potent than wild-type Noc (Table 3). These results clearly indicate that [RK$^{14-15}$]Noc exhibits much more enhanced biological activity than expected from the receptor-binding assay, as reported previously.[17,26]

In the binding assay, Trp-substituted peptides [WR$^{14-15}$]Noc (**2**) and [WK$^{14-15}$]Noc (**3**) exhibited almost the same high binding potency as well as [RK$^{14-15}$]Noc (Table 3). They were approximately 3 times more potent than the wild-type Noc. However, when their ability to affect the receptor activation was evaluated in the GTPγS functional assay, it became clear that these [W^{14}, (R/K)^{15}]Noc analogues **2** and **3** showed much more enhanced biological activity than expected from the receptor-binding assay. The EC_{50} values of [WR$^{14-15}$]Noc and [WK$^{14-15}$]Noc were approximately 10 times smaller than that of wild-type Noc: that is, these analogues were 10 times stronger than wild-type Noc (Table 4). In addition to [RK$^{14-15}$]Noc, these analogues are more potentiated synergistically in the receptor activation than with wild-type Noc.

2.3. Trp-substitution at position 15 with no synergistic activity

Another series of Trp-substituted peptides, [RW$^{14-15}$]Noc (**5**) and [KW$^{14-15}$]Noc (**6**), also showed almost the same high receptor-binding activity (IC_{50} = ca. 0.3 nM) as that of [RK$^{14-15}$]Noc (**1**), [WR$^{14-15}$]Noc (**2**), and [WK$^{14-15}$]Noc (**3**) (Table 3). These Trp^{15}-containing Noc analogues were a few times more potent (approximately 2.4-fold) than the wild-type Noc. However, in the actual binding assays, they were judged to be definitely weaker than Trp^{14}-containing Noc analogues **2** and **3**, as shown in Table 3.

[RW$^{14-15}$]Noc and [KW$^{14-15}$]Noc were also stronger (approximately 4.2-fold) than the wild-type Noc in the GTPγS functional assay. There was a slightly greater enhancement (1.75-fold) than expected from the receptor-binding assay. However, this enhancement was much smaller than that observed for [RK$^{14-15}$]Noc (**1**), [WR$^{14-15}$]Noc (**2**), and [WK$^{14-15}$]Noc (**3**) (Table 3). These findings indicate that only the Trp substitution at position 14 in [(R/K)^{14}, (R/K)^{15}]Noc can retain an intrinsic synergistic potentiation.

Table 1
The sequence list of a series of Trp-containing nociceptin analogues

Peptide No.	Peptides	Sequences	Position of Trp
	Nociceptin (Noc)	FGGFTGARKSARKLANQ	–
1	[RK$^{14-15}$]Noc	FGGFTGARKSARKRKNQ	–
2	[WR$^{14-15}$]Noc	FGGFTGARKSARK**W**RNQ	14
3	[WK$^{14-15}$]Noc	FGGFTGARKSARK**W**KNQ	14
4	[W^{14}]Noc	FGGFTGARKSARK**W**ANQ	14
5	[RW$^{14-15}$]Noc	FGGFTGARKSARK**R**WNQ	15
6	[KW$^{14-15}$]Noc	FGGFTGARKSARK**K**WNQ	15
7	[W^{15}]Noc	FGGFTGARKSARKLWNQ	15

Bold letters indicate the Trp residue replaced. The amino acid residues underlined are basic amino acids Arg(=R) and Lys(=K).

Table 2
Synthetic yield and analytical data of a series of Trp-containing nociceptin analogues

	Peptides	Yield (%)	RP-HPLC retention time (min)	MALDI-TOF MS	
				Found (*m/z*)	Calcd (m+H$^+$)
2	[WR$^{14-15}$]Noc	43	28.1	1968.62	1968.45
3	[WK$^{14-15}$]Noc	45	28.7	1940.27	1940.44
5	[RW$^{14-15}$]Noc	54	28.3	1968.56	1968.45
6	[KW$^{14-15}$]Noc	68	28.8	1940.29	1940.44

Retention times of wild-type Noc and [RK$^{14-15}$]Noc were 29.8 and 25.4 min, respectively.

Table 3
Binding activity of wild-type nociceptin, [RK$^{14-15}$]nociceptin, and a series of Trp-containing nociceptin analogues to rat ORL1 receptors

Nociceptin analogues		Binding activity IC_{50} (nM)	Relative potency IC_{50} (Noc)/IC_{50} (**1–7**)
	Nociceptin	0.73 ± 0.04	1.00
1	[RK$^{14-15}$]Noc	0.21 ± 0.02	3.48
2	[WR$^{14-15}$]Noc	0.23 ± 0.05	3.17
3	[WK$^{14-15}$]Noc	0.25 ± 0.03	2.92
4	[W^{14}]Noc	0.41 ± 0.04	1.78
5	[RW$^{14-15}$]Noc	0.30 ± 0.06	2.43
6	[KW$^{14-15}$]Noc	0.31 ± 0.04	2.35
7	[W^{15}]Noc	2.1 ± 0.04	0.35

Data are mean ± SEM of at least three experiments (n = 8–10).

Table 4
GTPγS binding activity of wild-type nociceptin, [RK$^{14-15}$]nociceptin, and a series of Trp-containing nociceptin analogues to rat ORL1 receptors

Nociceptin analogues		GTPγS binding activity EC_{50} (nM)	Relative potency EC_{50} (Noc)/EC_{50} (**1–7**)
	Nociceptin	13 ± 0.4	1.00
1	[RK$^{14-15}$]Noc	1.1 ± 0.08	11.8
2	[WR$^{14-15}$]Noc	1.3 ± 0.19	10.0
3	[WK$^{14-15}$]Noc	1.3 ± 0.12	10.0
4	[W^{14}]Noc	5.8 ± 1.1	2.24
5	[RW$^{14-15}$]Noc	3.1 ± 0.16	4.19
6	[KW$^{14-15}$]Noc	3.2 ± 0.14	4.06
7	[W^{15}]Noc	50 ± 2.9	0.26

Data are mean ± SEM of at least three experiments (n = 6–8).

3. Discussion

We have previously demonstrated that [RK$^{14-15}$]Noc, [KR$^{14-15}$]Noc, [RR$^{14-15}$]Noc, and [KK$^{14-15}$]Noc are all significantly potent both in the receptor-binding assay and in the GTPγS assay.[17,26] These analogues exhibited greater activity enhancement than that with the wild-type Noc, showing much more enhanced biological activity than expected from the receptor-binding assay. This increase in activity was brought about by placement of a combination of basic amino acid pairs in positions 14–15, where a Leu-Ala dipeptide unit is located in wild-type Noc. Since the single replacement of Leu^{14}-Ala^{15} with Arg or Lys generated analogues exhibiting no extra enhancement of biological activity, it appears that the optimal effect in enhancing the receptor activation requires basic Arg and/or Lys residues at adjacent positions 14–15. The highly enhanced biological activity of [(R/K)^{14}, (R/K)^{15}]Noc results from a kind of additional sympathetic interaction with the receptor.[26]

We have also shown previously that the activity enhancement induced by Arg and Lys at position 14 can be mimicked with the aromatic amino acid Trp.[26] [W^{14}]Noc was approximately twofold more potent than wild-type Noc in the binding assay (Table 3), and also approximately twofold more potent than wild-type Noc in the GTPγS functional assay (Table 4). Thus, [W^{14}]Noc was shown to exhibit an activity enhancement just as expected from its receptor-binding activity. A similar enhancement was attained with [R^{14}]Noc, [K^{14}]Noc, [R^{15}]Noc, and [K^{15}]Noc (Fig. 1).[26] These results strongly suggested that Trp^{14} would provide highly enhanced biological activity if the basic amino acid Arg or Lys was placed at position 15.[26] This enhancement was in fact evidenced in the present study.

As seen for [(R/K)^{14}, (R/K)^{15}]Noc, namely, [RK$^{14-15}$]Noc, [KR$^{14-15}$]Noc, [RR$^{14-15}$]Noc, and [KK$^{14-15}$]Noc, Trp^{14}-substituted analogues [WR$^{14-15}$]Noc (**2**) and [WK$^{14-15}$]Noc (**3**) were 3 times more potent than wild-type Noc in the receptor-binding assay (Table 3), and approximately 10 times stronger than wild-type Noc in the GTPγS functional assay (Table 4). Thus, as expected above, analogues **2** and **3** exhibited approximately three times greater activity enhancement than expected from the receptor-binding assay. Apparently, placing either Arg or Lys at position 15 for [W^{14}]Noc provides a distinct synergistic potentiation. In other words, the Trp substitution of Arg or Lys in position 14 of [(R/K)^{14}, (R/K)^{15}]Noc resulted in retention of the synergistic potentiation (Fig. 1).

Figure 1. Amino acid sequences of nociceptin and its highly potent analogues. All the amino acids are denoted in the one-letter code and basic amino acids Arg(=R) and Lys(=K) are placed in the gray box. At positions 14–15, original dipeptide LA was replaced by a series of basic dipeptides or Trp(=W)-containing dipeptides WR/WK, resulting in the effect of synergistic potentiation. Single replacements by Arg, Lys, or Trp at position 14 resulted in a rational normal potentiation, but not synergistic potentiation.

Such synergistic potentiation was not observed for the Trp substitution at position 15. Originally, [W^{15}]Noc was approximately a third as potent than wild-type Noc in the binding assay (Table 3), and also approximately a quarter as potent than wild-type Noc in the GTPγS functional assay (Table 4). Apparently, Trp^{15} is disadvantageous, resulting in a clear negative effect on the activities of [(R/K)^{14}, W^{15}]Noc. Although [RW$^{14-15}$]Noc (**5**) and [KW$^{14-15}$]Noc (**6**) showed receptor-binding activity increased to a few times greater than the wild-type Noc, these elicited no activity enhancement greater than that expected from the receptor-binding results in the GTPγS functional assay (Tables 3 and 4). Compounds **5** and **6** were only a few times stronger than the wild-type Noc. It was evident that the activity enhancement induced by Arg and Lys at position 15 cannot be mimicked with the aromatic amino acid Trp.

When we compare the IC_{50} and EC_{50} values of each Noc peptide, it is evident that all the peptides are less potent in the GTPγS functional assay than expected from their receptor-binding affinities. The estrangement between the IC_{50} and the EC_{50} values is largest for wild-type Noc itself (approximately 18-fold), which means that wild-type Noc has an imbalance in the efficiency of its receptor activities. The estrangement was improved in compounds **5** and **6** by approximately 70%, and then in compounds **1**, **2**, and **3** by approximately 230%. Certainly, these improvements were attained as a result of the placement of Arg, Lys, and/or Trp at positions 14 and 15. It should be noted, however, that even highly potent **1**, **2**, and **3** still exhibit an approximately fivefold estrangement between their receptor-binding activity and biological activity (Tables 3 and 4). Nociceptin itself appears to convey some kind of activity suppression, perhaps due to one of its characteristic suppressive functions such as hypoalgesia.

The present results clearly reveal that the structural roles of Arg/Lys residues are different, depending upon their positions at either 14 or 15. It is important to appreciate and understand that Arg/Lys is replaceable with Trp at position 14, but not at position 15. The only structural element that Arg, Lys, and Trp have in common is that they can potentially interact with aromatic residues such as Tyr, Trp, His, and Phe. In fact, Arg and Lys can interact with these aromatic amino acids by a cation/π interaction, while Trp interacts with them via a π/π hydrophobic interaction. It is thus highly likely that Arg, Lys, and Trp interact with aromatic receptor residue(s). On the other hand, Arg or Lys at position 15 must be in a favorable electrostatic interaction with acidic receptor residue(s).

The two RK repeats (RK$^{8-9}$ and RK$^{12-13}$) of wild-type Noc interact by electrostatic interactions with a receptor acidic region present in the second extracellular loop of ORL1.[14,15,28] It is now probable that the newly incorporated dipeptides at positions 14–15 such as WR, WK, RK, RR, KR, and KK allows wild-type Noc to establish additional interactions. Trp, Arg, or Lys placed at position 14 would lead to a π/π or cation/π interaction with nearby aromatic residues present in the ORL1 receptor, and simultaneously Arg or Lys placed at position 15 would guide the electrostatic interaction with an acidic receptor residue (Fig. 2). These extra interactions may stabilize the total ligand/receptor interaction, thus improving the ligand activity and resulting in a synergistic potentiation. Identification of the receptor-binding site for dipeptide$^{14-15}$ by a site-directed receptor mutagenesis study is now underway in our laboratory.

4. Conclusion

Hyperalgesic neuropeptide wild-type Noc becomes highly potent when a dipeptide unit RK, KR, RR, or KK is placed at positions

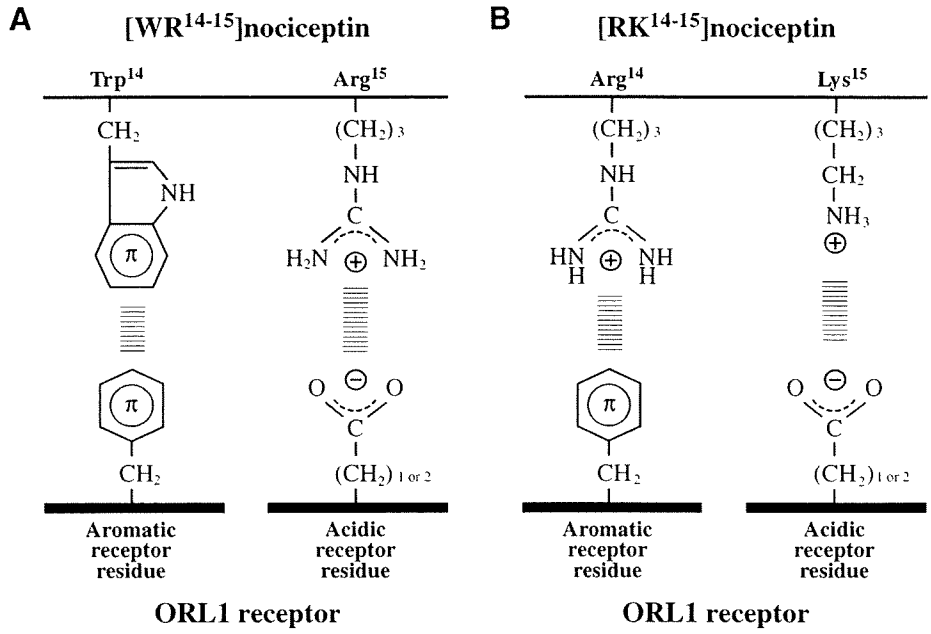

Figure 2. The structural looks of putative residual receptor–ligand interactions. (**A**) The π/π interaction between the receptor aromatic residue and the nociceptin-Trp^{14} residue in $[WR^{14-15}]$Noc together with the electrostatic interaction between the receptor acidic residue and the nociceptin-Arg^{15} residue. (**B**) The cation/π interaction between the receptor aromatic residue and the Arg^{14} residue in $[RK^{14-15}]$Noc together with the electrostatic interaction between the receptor acidic residue and the nociceptin-Lys^{15} residue.

14–15, where Leu-Ala is originally present. The resulting $[(R/K)^{14}, (R/K)^{15}]$Noc exhibited much more enhanced biological activity than expected from its receptor-binding activity. In the present study, this synergistic enhancement in biological activity or receptor activation was found to also occur when Trp replaced basic amino acids at position 14, but not at position 15. These results suggest the presence of a π interaction with the receptor aromatic residue and an electrostatic interaction with the acidic receptor residue.

5. Experimental

5.1. Peptide syntheses

All the peptides were synthesized by manual solid peptide syntheses or an automated peptide synthesizer ABI 433A (Applied Biosystems Inc., Foster City, CA) with the Fmoc synthetic strategy (0.1 mmol scale). Peptides were liberated from the resin using Reagent K (82.5% trifluoroacetic acid (TFA), 5% water, 5% thioanisole, 5% phenol, and 2.5% 1,2-ethanedithiol) at room temperature. After 3 h, the reaction was terminated with diethyl ether. The purification was carried out by reversed-phase HPLC (RP-HPLC) on a preparative column (25 × 250 mm, Cica-Merck LiChrospher RP-18 (e), 5 μm) with a linear gradient of 0.1% TFA and 80% acetonitrile containing 0.1% TFA. Detection was carried out at 230 nm. The fractions containing pure peptides were lypophilized, and the purity was verified by analytical RP-HPLC (4 × 250 mm, Cica-Merck LiChrospher 100 RP-18, 5 μm). Mass spectra of peptides were measured on a mass spectrometer Voyager™ DE-PRO (PerSeptive Biosystems Inc., Framingham, MA) with the matrix-assisted laser desorption ionization time-of-flight (MALDI-TOF) method.

5.2. Expression plasmid, cell culture, transfection, and membrane preparation

The cDNA clone of the rat ORL1 receptor was inserted into a pcDNA3 expression vector (Invitrogen, San Diego, CA) at the *Not*I/*Xba*I sites. COS-7 cells were maintained in Dulbecco's modified Eagle's medium supplemented with 10% fetal bovine serum and suitable antibiotics in a 5% CO_2 atmosphere at 37 °C. Plasmid DNA (30 μg) was transiently transfected into confluent COS-7 cells on a 150-cm^2-culture plate using the DEAE-dextran method. After 48 h, cells were harvested and centrifuged for 10 min at 500 *g* (4 °C). Cells were resuspended in 5 mM Tris buffer containing 1 mM EGTA and 11% saccharose (pH 7.4), and homogenized with the Teflon tissue homogenizer. The homogenate was centrifuged for 10 min at 1000 *g* (4 °C). The supernatant was recentrifuged for 20 min at 40,000 *g* (4 °C), and the pellet was washed with 5 mM Tris buffer containing 1 mM EGTA (pH 7.4). The concentration of membrane protein was estimated by the bicinchoninic acid (BCA) protein assay method using bicinchoninic acid (Pierce, Rockford, IL). The prepared membrane was frozen at −80 °C until use.

5.3. Radio-ligand receptor-binding assay

For the saturation-binding assay, a series of reaction mixtures containing 5 μg/ml membrane protein were incubated with increasing concentrations of [^{3}H]Noc (158 Ci/mmol, Amersham Pharmacia Biotech, Buckinghamshire, UK) (0.05–2 nM) for 90 min at 25 °C in 50 mM HEPES-Tris buffer (pH 7.4) containing 0.1% BSA. Bacitracin (100 μg/ml) was added as an enzyme inhibitor. After incubation, each incubation mixture (500 μl) was filtered through glass fiber filters (GF/B; Whatman Inc., Clifton, NJ), which were presteeped with 0.5% ethylene imine polymer for 1 h, and rinsed twice with 50 mM Tris–HCl buffer (pH 7.4). Non-specific binding was determined in the presence of 10 μM wild-type Noc. The receptor-binding potencies of the synthetic peptides were assessed by competitive binding assay. Briefly, membranes (5 μg/ml), serial concentrations of synthetic peptide, and 0.05 nM [^{3}H]Noc were incubated for 90 min at 25 °C in the same buffer (2 ml in each tube). The computer program ALLFIT[29] was used to draw dose–response curves for the analysis. The binding potency of each peptide was estimated as the IC_{50} value, the peptide concentration at which the half-maximal inhibition is achieved.

5.4. In vitro [^{35}S]GTPγS-binding assays

The in vitro biological activities of the synthetic peptides were appraised by [^{35}S]GTPγS-binding assay. The membranes (5 μg) were suspended in 50 mM HEPES-Tris buffer (pH 7.4) containing 100 mM NaCl, 10 mM $MgCl_2$, 200 mM EGTA, and 200 μM dithiothreitol. Bacitracin (100 μg/ml) was added as an enzyme inhibitor. Each tube (100 μl) was incubated for 60 min at 25 °C with the appropriate concentration of peptides in the presence of 3 μM GDP and 100 pM of [^{35}S]GTPγS (1000 Ci/mmol; Amersham Pharmacia Biotech). Non-specific binding was determined in the presence of 10 μM GTPγS. After incubation, each mixture was filtered through glass fiber filters (GF/B; Whatman) and rinsed in the same manner as described for the radio-ligand receptor-binding assay. The functional activity was estimated as EC_{50}, that is, the peptide concentration generating 50% of the maximal observed stimulation of GTPγS binding.

Acknowledgements

This study was supported in part by Health and Labor Sciences Research Grants to Y.S., for Research on the Risk of Chemical Substances, from the Ministry of Health, Labor, and Welfare of Japan. This work was also supported in part by grants-in-aid from the Ministry of Education, Culture, Sports, Science, and Technology of Japan to Y.S.

References and notes

1. Meunier, J. C.; Mollereau, C.; Toll, L.; Suaudeau, C.; Moisand, C.; Alvinerie, P.; Butour, J. L.; Guillemot, J. C.; Ferrara, P.; Monsarrat, B. *Nature* **1995**, *377*, 532.
2. Reinscheid, R. K.; Nothacker, H. P.; Bourson, A.; Ardati, A.; Henningsen, R. A.; Bunzow, J. R.; Grandy, D. K.; Langen, H.; Monsma, F. J., Jr.; Civelli, O. *Science* **1995**, *270*, 792.
3. Mollereau, C.; Parmentier, M.; Mailleux, P.; Butour, J. L.; Moisand, C.; Chalon, P.; Caput, D.; Vassart, G.; Meunier, J. C. *FEBS Lett.* **1994**, *341*, 33.
4. Chen, Y.; Fan, Y.; Liu, J.; Mestek, A.; Tian, M.; Kozak, C. A.; Yu, L. *FEBS Lett.* **1994**, *347*, 279.
5. Wang, J. B.; Johnson, P. S.; Imai, Y.; Persico, A. M.; Ozenberger, B. A.; Eppler, C. M.; Uhl, G. R. *FEBS Lett.* **1994**, *348*, 75.
6. Nishi, M.; Takeshima, H.; Mori, M.; Nakagawara, K.; Takeuchi, T. *Biochem. Biophys. Res. Commun.* **1994**, *205*, 1353.
7. Sandin, J.; Georgieva, J.; Schott, P. A.; Ogren, S. O.; Terenius, L. *Eur. J. Neurosci.* **1997**, *9*, 194.
8. Manabe, T.; Noda, Y.; Mamiya, T.; Katagiri, H.; Houtani, T.; Nishi, M.; Noda, T.; Takahashi, T.; Sugimoto, T.; Nabeshima, T.; Takeshima, H. *Nature* **1998**, *394*, 577.
9. Jenck, F.; Moreau, J. L.; Martin, J. R.; Kilpatrick, G. J.; Reinscheid, R. K.; Monsma, F. J., Jr.; Nothacker, H. P.; Civelli, O. *Proc. Natl. Acad. Sci. U.S.A.* **1997**, *94*, 14854.
10. Thomsen, C.; Hohlweg, R. *Br. J. Pharmacol.* **2000**, *131*, 903.
11. Wichmann, J.; Adam, G.; Rover, S.; Hennig, M.; Scalone, M.; Cesura, A. M.; Dautzenberg, F. M.; Jenck, F. *Eur. J. Med. Chem.* **2000**, *35*, 839.
12. Dooley, C. T.; Houghten, R. A. *Life Sci.* **1996**, *59*, PL23.
13. Reinscheid, R. K.; Ardati, A.; Monsma, F. J., Jr.; Civelli, O. *J. Biol. Chem.* **1996**, *271*, 14163.
14. Topham, C. M.; Mouledous, L.; Poda, G.; Maigret, B.; Meunier, J. C. *Protein Eng.* **1998**, *11*, 1163.
15. Mollereau, C.; Mouledous, L.; Lapalu, S.; Cambois, G.; Moisand, C.; Butour, J. L.; Meunier, J. C. *Mol. Pharmacol.* **1999**, *55*, 324.
16. Zhang, C.; Miller, W.; Valenzano, K. J.; Kyle, D. J. *J. Med. Chem.* **2002**, *45*, 5280.
17. Okada, K.; Sujaku, T.; Chuman, Y.; Nakashima, R.; Nose, T.; Costa, T.; Yamada, Y.; Yokoyama, M.; Nagahisa, A.; Shimohigashi, Y. *Biochem. Biophys. Res. Commun.* **2000**, *278*, 493.
18. Rizzi, D.; Rizzi, A.; Bigoni, R.; Camarda, V.; Marzola, G.; Guerrini, R.; De Risi, C.; Regoli, D.; Calo, G. *J. Pharmacol. Exp. Ther.* **2002**, *300*, 57.
19. Broccardo, M.; Linari, G.; Guerrini, R.; Agostini, S.; Petrella, C.; Improta, G. *Peptides* **2005**, *26*, 1590.
20. Calo, G.; Rizzi, A.; Rizzi, D.; Bigoni, R.; Guerrini, R.; Marzola, G.; Marti, M.; McDonald, J.; Morari, M.; Lambert, D. G.; Salvadori, S.; Regoli, D. *Br. J. Pharmacol.* **2002**, *136*, 303.
21. McDonald, J.; Calo, G.; Guerrini, R.; Lambert, D. G. *Arch. Pharmacol.* **2003**, *367*, 183.
22. Carra, G.; Rizzi, A.; Guerrini, R.; Barnes, T. A.; McDonald, J.; Hebbes, C. P.; Mela, F.; Kenigs, V. A.; Marzola, G.; Rizzi, D.; Gavioli, E.; Zucchini, S.; Regoli, D.; Morari, M.; Salvadori, S.; Rowbotham, D. J.; Lambert, D. G.; Kapusta, D. R.; Calo, G. *J. Pharmacol. Exp. Ther.* **2005**, *312*, 1114.
23. Calo, G.; Guerrini, R.; Rizzi, A.; Salvadori, S.; Burmeister, M.; Kapusta, D. R.; Lambert, D. G.; Regoli, D. *CNS Drug Rev.* **2005**, *11*, 97.
24. Chiou, L. C.; Liao, Y. Y.; Guerrini, R.; Calo, G. *Eur. J. Pharmacol.* **2005**, *515*, 47.
25. Peng, Y. L.; Chang, M.; Dong, S. L.; Li, W.; Han, R. W.; Fu, G. X.; Chen, Q.; Wang, R. *Regul. Pept.* **2006**, *134*, 75.
26. Okada, K.; Isozaki, K.; Li, J.; Matsushima, A.; Nose, T.; Costa, T.; Shimohigashi, Y. *Bioorg. Med. Chem.* **2008**, *16*, 9261.
27. Okada, K.; Sujaku, T.; Nakashima, R.; Nose, T.; Yamada, Y.; Yokoyama, M.; Nagahisa, A.; Shimohigashi, Y. *Bull. Chem. Soc. Jpn.* **1999**, *72*, 1899.
28. Dooley, C. T.; Spaeth, C. G.; Berzetei-Gurske, I. P.; Craymer, K.; Adapa, I. D.; Brandt, S. R.; Houghten, R. A.; Toll, L. *J. Pharmacol. Exp. Ther.* **1997**, *283*, 735.
29. DeLean, A.; Munson, P. J.; Rodbard, D. *Am. J. Physiol.* **1978**, *235*, E97.

Peptide Science 2009: K. Okamoto (Ed.)
The Japanese Peptide Society (2010)

The Agonist/Antagonist Differential-docking Screening (AADS) Method for Exploration of the Estrogen Receptor-binding Chemicals

Takeru Nose, Takatoshi Tokunaga, and Yasuyuki Shimohigashi

Department of Chemistry, Faculty and Graduate School of Science, Kyushu University, Fukuoka, 812-8581, Japan
e-mail: nosescc@chem.kyushu-univ.jp

We have established a novel method to screen endocrine-disrupting chemicals by in silico *docking calculations, which utilized the both agonist-bound- and antagonist-bond-ligand binding domains as templates. This agonist/antagonist differential-docking screening (AADS) method predicted, for example, 4-(1-adamantyl) phenol as an agonist of the human estrogen receptor α. The AADS method is an approach that appears to foresee both the binding potency and the agonist or antagonist activity of chemicals for the target nuclear receptors.*

Keywords: agonist/antagonist differential-docking screening (AADS), docking calculation, nuclear receptor

Introduction

Nuclear receptors (NRs), which play a central role as transcription factors in various biological processes, consist of five domains: N-terminal domain, DNA-binding domain, hinge domain, ligand-binding domain (LBD), and C-terminal domain. In general, the LBD has a pocket to capture a chemical, which has agonist or antagonist activity [1]. Because the pocket, which was named ligand binding pocket (LBP), exists on the LBD, the LBD is considered to be the major binding site for the pharmacological agents and the endocrine disrupting chemicals (EDCs).

Currently, numerous industrial chemicals are suspected to be EDCs. If we could predict that the chemicals would bind to the LBP, it would definitely be advantageous for the design of agonists or antagonists of particular NR. It would also be very helpful to predict which chemicals would cause serious disruptions in the endocrine system. In this study, to establish a novel method that screens a huge number of chemicals to explore EDCs, the docking calculation procedure was newly developed by using one of NRs, the human estrogen receptor α (ERα). The ERα-LBD changes its conformation, depending upon the ligand docks as either agonist or antagonist. Such differences of the conformation were observed in 3D structures of ERα-LBD/ligand complexes, which determined by X-ray crystallography [2,3]. Therefore, we used two agonist-bound (PDB: 1ERE and 3ERD) and two another antagonist-bound (1ERR and 3ERT) ERα-LBD's crystal structures as templates for the docking calculation, and compared binding energies elucidated from

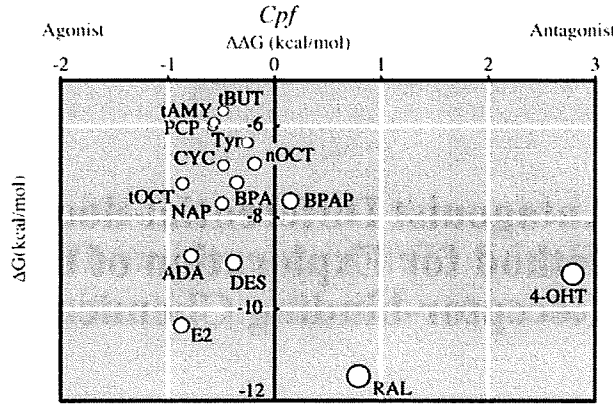

Fig. 1. Plotting analysis of the ADDS method.
ΔG versus ΔΔG plotting analysis. The size of each plot corresponds to the relative molecular size of the test chemical. Abbreviations of chemicals are denoted in parentheses: pentachlorophenol (PCP), 4-tert-butylphenol (tBUT), 4-tert-amylphenol (tAMY), 4-cyclohexylphenol (CYC), 4-n-octylphenol (nOCT), 4-tert-octylphenol (tOCT), bisphenol A (BPA), 4-(2-naphthyl)phenol (NAP), 4-(1-adamantyl)phenol (ADA), bisphenol AP (BPAP), 17β-estradiol (E2), dietylstilbestrol (DES), raloxifene (RAL), and 4-hydroxytamoxifen (4-OHT).

the docking calculations by using each template. This calculation method was named as the agonist/antagonist differential-docking screening (AADS) [4].

Results and Discussion

Docking calculations were carried out by the program Autodock 3.0 (The Scripps Research Institute) and tested 16 chemicals. The average binding energies (ΔG) of the chemicals were obtained from the results of the docking calculations using four LBDs. The agonist/antagonist factor (ΔΔG=Cpf: conformation preference factor) was calculated as the difference between ΔG from the docking calculations used by agonist-bound receptors and antagonist-bound receptors.

The calculated free energies of binding (ΔG) of the known ER-ligands, E2, DES, RAL and 4-OHT, ranged from –8.98 to –11.47 kcal/mol. Among test chemicals, there was only one putative antagonist (Fig. 1). Because of its small minus ΔΔG value, it is possible that BPAP has weak antagonist-like activity. On the other hand, we identified 4-(1-adamantyl) phenol (ADA) as a relatively strong agonist for hERα. ADA attained a binding energy (–8.84 kcal/mol) greater than that of the other test chemicals and it had a plus ΔΔG value. The AADS method successfully predicted that ADA is almost as active as DES (ΔG = –8.98 kcal/mol).

References

1. Olefsky, J.M. (2001) *J. Biol. Chem.*, **276**, 36863-36864.
2. Brzozowski, A.M., Pike, A.C., Dauter, Z., Hubbard, R.E., Bonn, T., Engstrom, O., Ohman, L., Greene, G.L., Gustafsson, J.A., and Carlquist, M. (1997) *Nature,* **389**, 753-758.
3. Shiau, A.K., Barstad, D., Loria, P.M., Cheng, L., Kushner, P.J., Agard, D.A., and Greene, G.L. (1998) *Cell,* **95**, 927-937.
4. Nose, T., Tokunaga, T., and Shimohigashi, Y., *Toxicol. Lett.*, (2009) in press.